Papers

doi:10.5697/oc.53-3.691
OCEANOLOGIA, 53 (3), 2011.
pp. 691–729.

Inherent optical properties of suspended particulate matter in the southern Baltic Sea*

KEYWORDS
Suspended particulate matter
Inherent optical properties
Light absorption
Scattering and backscattering coefficients of particles

Sławomir B. Woźniak
Justyna Meler
Barbara Lednicka
Agnieszka Zdun
Joanna Stoń-Egiert

Institute of Oceanology,
Polish Academy of Sciences,
Powstańców Warszawy 55, Sopot 81–712, Poland;

e-mail: woznjr@iopan.gda.pl

⋆corresponding author

Received 14 December 2010, revised 16 June 2011, accepted 17 June 2011.

Abstract

The inherent optical properties (IOPs) of suspended particulate matter and their relations with the main biogeochemical characteristics of particles have been examined in the surface waters of the southern Baltic Sea. The empirical data were gathered at over 300 stations in open Baltic Sea waters as well as in the coastal waters of the Gulf of Gdańsk. The measurements included IOPs such as the absorption coefficient of particles, absorption coefficient of phytoplankton, scattering and backscattering coefficients of particles, as well as biogeochemical characteristics of suspended matter such as concentrations of suspended particulate

* Financial support for this study was provided by research project grant No. N306 2838 33 awarded to S. B. Woźniak by the Polish Ministry of Science and Higher Education and by Statutory Research Programme No. I.1 at the Institute of Oceanology, Polish Academy of Sciences, Sopot, Poland.

matter (SPM), particulate organic matter (POM), particulate organic carbon (POC) and chlorophyll *a* (Chl *a*). Our data documented the very extensive variability in the study area of particle concentration measures and IOPs (up to two orders of magnitude). Although most of the particle populations encountered were composed primarily of organic matter (av. POM/SPM = ca 0.8), the different particle concentration ratios suggest that the particle composition varied significantly. The relations between the optical properties and biogeochemical parameters of suspended matter were examined. We found significant variability in the constituent-specific IOPs (coefficients of variation (CVs) of at least 30% to 40%, usually more than 50%). Simple best-fit relations between any given IOP versus any constituent concentration parameter also highlighted the significant statistical errors involved. As a result, we conclude that for southern Baltic samples an easy yet precise quantification of particle IOPs in terms of the concentration of only one of the following parameters – SPM, POM, POC or Chl *a* – is not achievable. Nevertheless, we present a set of best statistical formulas for a rough estimate of certain seawater constituent concentrations based on relatively easily measurable values of seawater IOPs. These equations can be implemented in practice, but their application will inevitably entail effective statistical errors of estimation of the order of 50% or more.

1. Introduction

One of the important issues in the marine sciences is to study the relationships between seawater constituents and their optical properties in different regions of world oceans and seas (Dera 1992, 2003). On the one hand, elementary optical processes such as light absorption and scattering by different seawater constituents determine how sunlight is propagated and utilized in water, which has a great influence on the thermal regimes and states of marine ecosystems (Trenberth (ed.) 1992, Kirk 1994). On the other hand, armed with a knowledge of seawater optical properties, we may be able to identify the composition and concentrations of different seawater constituents. An understanding of the relations between these constituents and their optical properties is thus necessary for both the ecological and climate modelling of marine environments and also for establishing practical marine research methods. These interrelations are especially complicated with respect to oceanic shelf regions and also to enclosed and semi-enclosed seas, jointly described as case II waters according to the classification by Morel & Prieur (1977). As opposed to open ocean waters (classified as case I waters and whose optical properties are relatively well studied), in water bodies classified as case II, both autogenic (e.g. phytoplankton and its degradation products) and allogenic (substances transported from land by rivers, or by wind, and substances resuspended from the sea bottom and eroded from shorelines) constituents may play an important role, and their concentrations may be uncorrelated with one another.

For decades laboratory biogeochemical analyses of discrete water samples collected at sea have been used to determine the types and concentrations of suspended and dissolved substances in seawater. But such analyses are usually laborious and time-consuming and so are difficult to apply on a large scale. Another widely used tool for the monitoring and research of oceans and seawaters is remote sensing (see e.g. Arst 2003). Performed from above the sea surface (from a ship, aircraft or earth satellite platform), these measurements are based on analyses of the remote sensing reflectance spectrum (one of the so-called apparent optical properties (AOPs)), also commonly referred to as 'ocean colour'. Unlike classic laboratory analyses of discrete water samples, remote sensing allows the marine environment to be investigated at large spatial and temporal scales, but it also comes at the cost of certain irreducible limitations. Remote sensing is feasible only in suitable meteorological conditions, and the signal reaching the remote instrument always has to be corrected for 'noise' coming from the Earth's atmosphere owing to the presence of water vapour, aerosols and other constituents scattering and absorbing solar radiation. Furthermore, the object of remote sensing observations may be only the surface layers of water basins, and this seems to be the greatest limitation. In addition, the physical interpretation of reflectance spectra requires a thorough understanding of the complicated relations involved, namely, a) how concentrations and types of seawater constituents influence the inherent optical properties (IOPs), i.e. the absorption and scattering of light, and b) how the latter in certain ambient light field conditions affects different apparent optical properties (AOPs) such as remote sensing reflectance (Gordon et al. 1975, Gordon 2002). Therefore, an ever greater depth of understanding of the relationships between seawater constituents and seawater IOPs is required for the development of ever more precise remote sensing algorithms linking seawater AOPs with the presence of different constituents in marine environments.

Studies of the relations between constituents and IOPs are also important, because they may lead to improved direct in situ optical (IOP based) methods for environmental research and monitoring. It would appear that these methods still possess a latent potential for the field estimation of biogeochemical properties of suspended particulate matter. Suspended substances, as opposed to dissolved ones, not only absorb light but also scatter it. For this reason marine suspensions leave unique 'fingerprints' on seawater IOPs, which at least in theory should enable them to be identified qualitatively and quantitatively. With IOPs being measured directly using suitable identification algorithms, it should be possible to achieve a conspicuous improvement in the spatial and temporal

resolution of suspended matter field studies as compared to classical biogeochemical analyses of discrete water samples. In some respects direct optical measurements may also offer a valuable alternative to situations when remote sensing is inapplicable for some reason.

Whereas the optical properties of open ocean waters (mostly dominated by organic autogenic substances) have been a popular research subject among the marine optics community for many decades (see e.g. Morel & Maritorena (2001) and the list of works cited there), comprehensive in situ studies of the relations between the types and concentrations of suspended organic and inorganic matter and seawater IOPs in case II waters have been few and far between and have only begun to intensify in the last ten years or so. An example of the latter is the work by Babin et al. (2003a,b), who report on the variability ranges of absorption and scattering coefficients in relation to the concentration of suspended particulate matter (SPM) and the concentration of phytoplankton pigments in different coastal waters around Europe (including the south-western Baltic Sea). Further field studies in the optically complex case II waters have been carried out by Green et al. (2003) (the New England shelf), Gallegos et al. (2005) (a shallow embayment in Chesapeake Bay), McKee & Cunningham (2006) (Irish Sea shelf waters), Oubelkheir et al. (2006) (tropical coastal waters of eastern Australia), Vantrepotte et al. (2007) (eastern English Channel), Snyder et al. (2008), Stavn & Richter (2008) (coastal waters off New Jersey, the northern Gulf of Mexico, and Monterey Bay) and Woźniak et al. (2010) (southern California coastal waters). These examples show that the question of suspended matter optical properties in case II waters is still an open scientific problem. As far as the Baltic Sea (another case II water body) is concerned, different aspects of the penetration of light into its waters have been studied by various authors for the past 50 years (see Dera & Woźniak (2010) and the list of the works cited there), but even so, the subject of suspended matter optical properties in the Baltic has not received the attention it merits.

In this study we report on experimental data collected in the southern part of the Baltic Sea. Our primary objective is to examine the variability in the inherent optical properties of suspended matter (the light absorption coefficients of particles, the absorption coefficients of phytoplankton, and the scattering and backscattering coefficients of particles) and their relations with key biogeochemical characteristics describing particle populations (such as concentrations of suspended particulate matter (SPM), particulate organic matter (POM), particulate organic carbon (POC) and chlorophyll *a* (Chl *a*)). This has been done mainly through statistical analyses of the variability of constituent-specific IOPs (i.e. IOPs normalized to certain

concentrations of constituents) and also by deriving simple statistical best-fit equations parameterizing the IOPs in terms of the concentrations of selected seawater constituents. In addition, we discuss the possibility of retrieving biogeochemical characteristics from particle IOPs: with a set of simple formulas and procedures, measured particulate IOPs can be used to work out a rough estimate of suspended matter biogeochemical characteristics.

2. Methods

2.1. Sampling

The optical and biogeochemical properties of suspended matter in the surface waters of the southern Baltic Sea were examined. The empirical data were gathered at over 300 stations during 15 short cruises on board r/v 'Oceania' between August 2006 and September 2009 (in late winter and spring (March, April, May) and in late summer and autumn (August, September, October, November)). The study area covered the open waters of the southern Baltic as well as the coastal regions of the Gulf of Gdańsk (see Figure 1). At each station the light scattering properties of seawater (the scattering and backscattering coefficients, and volume scattering function) and salinity were measured in situ in the surface layer (down to 1.5 m depth; see below for details). Samples of surface seawater were also taken with 20 L Niskin bottles for laboratory measurements of

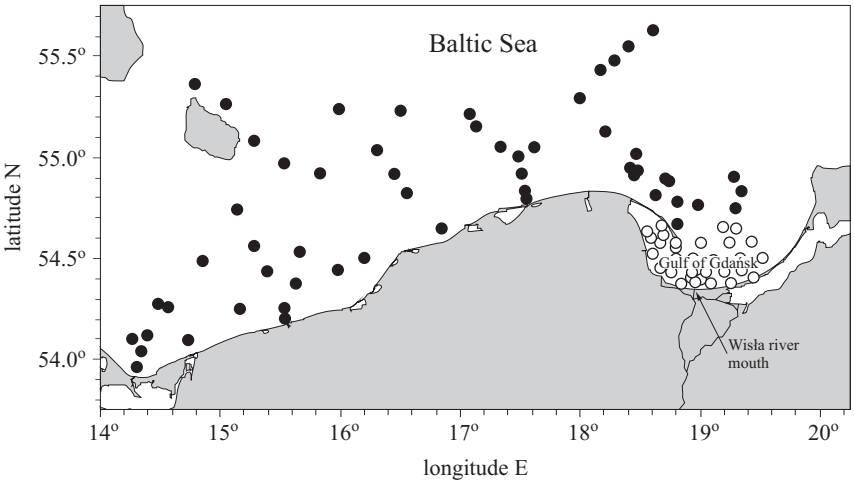

Figure 1. Location of sampling stations. Stations located in the open waters of the southern Baltic Sea are denoted by black dots, those in the Gulf of Gdańsk by open circles

light absorption properties (absorption coefficients of suspended particles, and coloured dissolved organic matter (CDOM)) and for analysis of different biogeochemical properties of suspended matter.

2.2. Concentrations of seawater constituents

The concentration of suspended particulate matter, SPM (units are g m^{-3}), defined as the dry mass of particles per unit volume of water, was determined using a standard gravimetric technique. We used specially prepared GF/F filters (25 mm in diameter) pre-combusted for 4 h at 450°C, pre-washed with pure deionized and particle-free water (to prevent the loss of filter material during the filtration of the main sample), then dried and pre-weighed. Measured volumes of seawater (between 150 and 1500 mL) were filtered immediately after sample collection. At the end of filtration, the filters were rinsed with about 60 mL of deionized water to remove sea salt. Separate tests showed that such rinsing volumes efficiently removed sea salt from southern Baltic Sea water, which has a relatively low salinity (the salinity of our samples ranged from 0.6 to 8.3 PSU (av. = 6.9 PSU)). The filters with their particle load were dried and stored in a freezer for later analysis. The dry mass of particles collected on the filters was measured with a Radwag WAX110 microbalance (resolution 0.01 mg). Three replicate filters were measured in each sample, with the reproducibility generally within ± 17%.

Having been analysed for SPM concentration, the filters were combusted for 4 h at 450°C to remove the organic particle fraction (loss on ignition (LOI) technique; see e.g. Pearlman et al. (1995)), then reweighed. The difference in weight before and after combustion yielded the concentration of particulate organic matter (POM) [g m^{-3}]. The reproducibility of replicate measurements was generally within ± 16%.

Particles were also collected at sea by filtration using separate sets of pre-combusted GF/F filters (three replicates per experiment) for the analysis of the particulate organic carbon (POC) concentration [g m^{-3}]. The sample filters were dried after filtration and stored until analysis by high temperature combustion (Perkin Elmer CHN 2400). The reproducibility of the POC replicate measurements was generally within ± 19%.

Samples were also taken for the analysis of phytoplankton pigment concentrations. Particles collected on GF/F filters were stored in liquid nitrogen and later analysed on land by HPLC (see Stoń-Egiert & Kosakowska 2005, Stoń-Egiert et al. 2010). More than 20 different pigments were identified with this technique. Later in this paper we will refer to the total concentration of chlorophyll *a*, Chl *a* [mg m^{-3}] (sum of chlorophyll *a*, allomer and epimer, chlorophyllid *a* and phaeophytin *a*) and the concentration

of total accessory pigments [mg m^{-3}] (the sum of the following pigments: chlorophyll *b*, chlorophyll $c_1 + c_2$, chlorophyll c_3, peridinin, 19'but-fucoxanthin, fucoxanthin, 19'hex-fucoxathin, prasinoxanthin, canthaxanthin, echinenone, α-carotene, neoxanthin, violaxanthin, diadinoxanthin, antheraxanthin, alloxanthin, diatoxanthin, zeaxanthin, lutein, β-carotene, aphanizophyll, myxoxanthophyll).

2.3. Inherent optical properties of seawater

Particulate absorption spectra, $a_p(\lambda)$ [m^{-1}], were measured in the 350–750 nm spectral range with a Unicam UV4-100 spectrophotometer equipped with an integrating sphere (66 mm diameter). The Transmission-Reflectance (T-R) filter-pad technique was used (Tassan & Ferrari 1995, 2002). For a given sample, this technique requires optical density spectra to be measured with at least four different filter-detector configurations involving sample and blank GF/F filters. From these optical densities, we calculated the desired value representing the optical density $OD_s(\lambda)$ of the particles collected on the filter following the equations of Tassan & Ferrari (1995, 2002). In these calculations we assumed that the transmittance of the sample filter was identical, regardless of whether the side of the filter with particles was facing the beam or not. This is a good assumption, as the procedure is thereby simplified by the avoidance of an additional transmittance measurement with the particles on the filter facing the entrance to the integrating sphere rather than the incident beam (Tassan & Ferrari 2002). The correction for the pathlength amplification factor (the so-called β-factor) was applied, in which the optical density of particles on the filter $OD_s(\lambda)$ was converted to the equivalent optical density of particles in suspension $OD_{sus}(\lambda)$ (e.g. Mitchell 1990). We used the formula $OD_{sus}(\lambda) = 0.592\,[OD_s(\lambda)]^2 + 0.4\,OD_s(\lambda)$, which is based on experiments with several phytoplankton cultures, mineral-rich particulate assemblages and natural assemblages of particles from marine environments (see Kaczmarek et al. 2003, Stramska et al. 2006). Finally, the particulate absorption coefficient $a_p(\lambda)$ was determined by multiplying $OD_{sus}(\lambda)$ by ln(10) and the clearance area of the filter, and dividing this product by the volume of sample filtered.

In order to partition $a_p(\lambda)$ into phytoplankton $a_{ph}(\lambda)$ and non-phytoplankton $a_d(\lambda)$ (commonly referred to as detritus) components, the sample GF/F filters were subjected to similar transmittance and reflectance measurements following treatment with $Ca(ClO)_2$ (Woźniak et al. 1999). In this treatment, the particles on the sample filter were exposed to a small amount of a 2% $Ca(ClO)_2$ solution for several minutes with the primary aim of bleaching the phytoplankton pigments. The T-R measurements

on the bleached sample filters yielded the estimates of $a_d(\lambda)$. The final spectral values of a_d were adjusted so that $a_d(750)$ was equal to $a_p(750)$. The phytoplankton absorption coefficient $a_{ph}(\lambda)$ was then obtained as the difference between $a_p(\lambda)$ and $a_d(\lambda)$.

We also measured the absorption coefficient of coloured dissolved organic matter $a_{\mathrm{CDOM}}(\lambda)$ [m^{-1}] using a Unicam UV4-100 spectrophotometer. These measurements were made in 5 cm cuvettes on samples filtered through a 0.2 μm acetate filter and relative to pure water (deionized and particle-free). The values of $a_{\mathrm{CDOM}}(\lambda)$ were calculated by multiplying the baseline-corrected optical densities $OD_{\mathrm{CDOM}}(\lambda)$ by ln(10) and dividing by the pathlength of 0.05 m. Assuming that $a_{\mathrm{CDOM}}(\lambda)$ is negligible at wavelengths roughly above 680 nm, any measured offset was subtracted to obtain the final $a_{\mathrm{CDOM}}(\lambda)$.

The scattering coefficients of particles $b_p(\lambda)$ [m^{-1}] were calculated as the difference between the spectral attenuation and absorption coefficients by non-water constituents (dissolved and particulate) – $c_n(\lambda)$ and $a_n(\lambda)$ respectively. The latter were measured in situ in the near-surface layer (ca 1.5 m depth) using a spectral absorption-attenuation meter (WET Labs ac-9) at nine wavelengths (412, 440, 488, 510, 532, 555, 650, 676, 715 nm) and a 25 cm pathlength. Corrections for in situ temperature and salinity effects on the optical properties of water were applied according to Pegau et al. (1997). A correction for the incomplete recovery of the scattered light in the absorption tube of the ac-9 instrument (the so-called proportional method) was used according to Zaneveld et al. (1994).

The backscattering coefficients of particles $b_{bp}(\lambda)$ [m^{-1}] were estimated from in situ measurements performed in the near-surface layer (ca 1.5 m depth) using a spectral backscattering meter (HOBI Labs Hydroscat-4) at four wavelengths (420, 488, 550 and 620 nm). The raw data from the instrument, i.e. values of volume scattering function at an angle of 140°, $\beta(140)$ were used for estimating b_{bp} according to the method described in Maffione & Dana (1997) and Dana & Maffione (2002). A correction for the incomplete recovery of backscattered light in highly attenuating waters (the so-called sigma-correction) was applied in accordance with the instrument User's Manual (HOBI Labs 2008) using data on absorption and attenuation coefficients measured with the ac-9 instrument.

The volume scattering functions of particles for a light wavelength of 532 nm, $\beta_{p,\,532}(\theta)$ [$\mathrm{m}^{-1}\ \mathrm{sr}^{-1}$], were also measured in situ in the near-surface layer of seawater for a portion of our samples (collected between April 2008 and September 2009). This was done with a WET Labs ECO volume scattering function meter at angles of 100, 125 and 150°. The raw data measured with this instrument were corrected for the dark counts of the

detector (determined at each station) and then calibrated according to the manufacturer's specification. The volume scattering function of pure water (according to Morel 1974) was then subtracted in order to obtain the values representing the volume scattering functions of particles, $\beta_{p,532}(\theta)$.

3. Results and discussion

3.1. General variability of suspended matter biogeochemical characteristics and IOPs

Our data from the southern Baltic Sea study area exhibit considerable variability in all the particle concentrations measured. In the case of the basic suspended particulate matter characteristic – its mass concentration (SPM) – the corresponding coefficient of variation (CV, defined as the ratio of the standard deviation to the average value and expressed as a percentage) is more than 90%. There is a >40-fold variability between the measured maximum and minimum values (see Table 1). In the case of other biogeochemical quantities like concentrations of POC and POM, which characterize the organic fraction of suspended matter, the recorded variability is of the same order (with CV reaching $>90\%$ in both cases, and with >50-fold and >30-fold variability between the extremes respectively). In the case of the phytoplankton pigment concentrations found within the suspended matter the variability is even greater. The concentration of the primary pigment, chlorophyll *a* (Chl *a*), has a CV of almost 130% and there is a >190-fold variability between the maximum and minimum values; the variability in the overall concentration of all accessory pigments is of the same order of magnitude.

Although most of the particle populations encountered were composed primarily of organic matter, the different particle concentration ratios suggest that particle composition varied significantly. For example, the average POM/SPM ratio is about 0.8 but the corresponding CV is 22% (see the data in Table 1). In the case of the two other composition ratios – POC/SPM (av. = ca 0.25) and Chl *a*/SPM (av. = ca 3.5×10^{-3}) – the corresponding CVs are even greater (41% and 81% respectively). As these three composition ratios can provide insight into the variable proportions between the organic and inorganic fractions in the total suspended matter, there are two other ratios worth mentioning, which suggest that the composition of the organic fraction of suspended matter is itself subject to significant variability. The CV of the Chl *a*/POC ratio (av. $= 1.3 \times 10^{-2}$) is 74%, while for the ratio of total accessory pigments to Chl *a* it is 29%. The relations between the different biogeochemical measures characterizing suspended matter are illustrated graphically in Figure 2. This also shows

Table 1. Variability range of different characteristics of suspended particulate matter and inherent optical properties

Parameter	Minimum value	Maximum value	Average value	Standard deviation (coefficient of variation)	Number of samples
SPM [g m^{-3}]	**0.359**	**15.7**	2.42	2.24 (93%)	293
POM [g m^{-3}]	**0.329**	**11.3**	1.86	1.77 (95%)	281
POC [g m^{-3}]	**0.075**	**3.93**	0.58	0.564 (97%)	174
Chl *a* [mg m^{-3}]	**0.381**	**72.6**	7.62	10.0 (131%)	335
total accessory pigments [mg m^{-3}]	**0.366**	**63.7**	5.14	6.36 (124%)	335
POM/SPM (g:g)	0.339	1.05	**0.795**	0.174 **(22%)**	281
POC/SPM (g:g)	0.0621	0.488	**0.252**	0.104 **(41%)**	142
Chl *a*/SPM (g:g)	2.5×10^{-4}	3.22×10^{-2}	$\mathbf{3.54 \times 10^{-3}}$	2.87×10^{-3} **(81%)**	286
Chl *a*/POC (g:g)	2.11×10^{-3}	7.54×10^{-2}	$\mathbf{1.35 \times 10^{-2}}$	9.92×10^{-3} **(74%)**	168
total accessory pigments/Chl *a* (g:g)	0.372	1.72	**0.761**	0.222 **(29%)**	335
$a_p(440)$ [m^{-1}]	**0.0686**	**3.24**	0.405	0.416 (103%)	332
$a_{ph}(440)$ [m^{-1}]	(below limit of detection)	**2.84**	0.292	0.32 (110%)	321
$a_d(440)$ [m^{-1}]	(below limit of detection)	**1.22**	0.115	0.142 (123%)	321
$b_p(555)$ [m^{-1}]	**0.224**	**9.27**	1.45	1.39 (96%)	260
$b_{bp}(420)$ [m^{-1}]	**0.00346**	**0.231**	0.0249	0.0295 (119%)	233
$\beta_{p,532}(100°)$ [m^{-1} sr^{-1}]	$\mathbf{4.91 \times 10^{-4}}$	$\mathbf{1.86 \times 10^{-2}}$	3.23×10^{-3}	3.22×10^{-3} (100%)	179

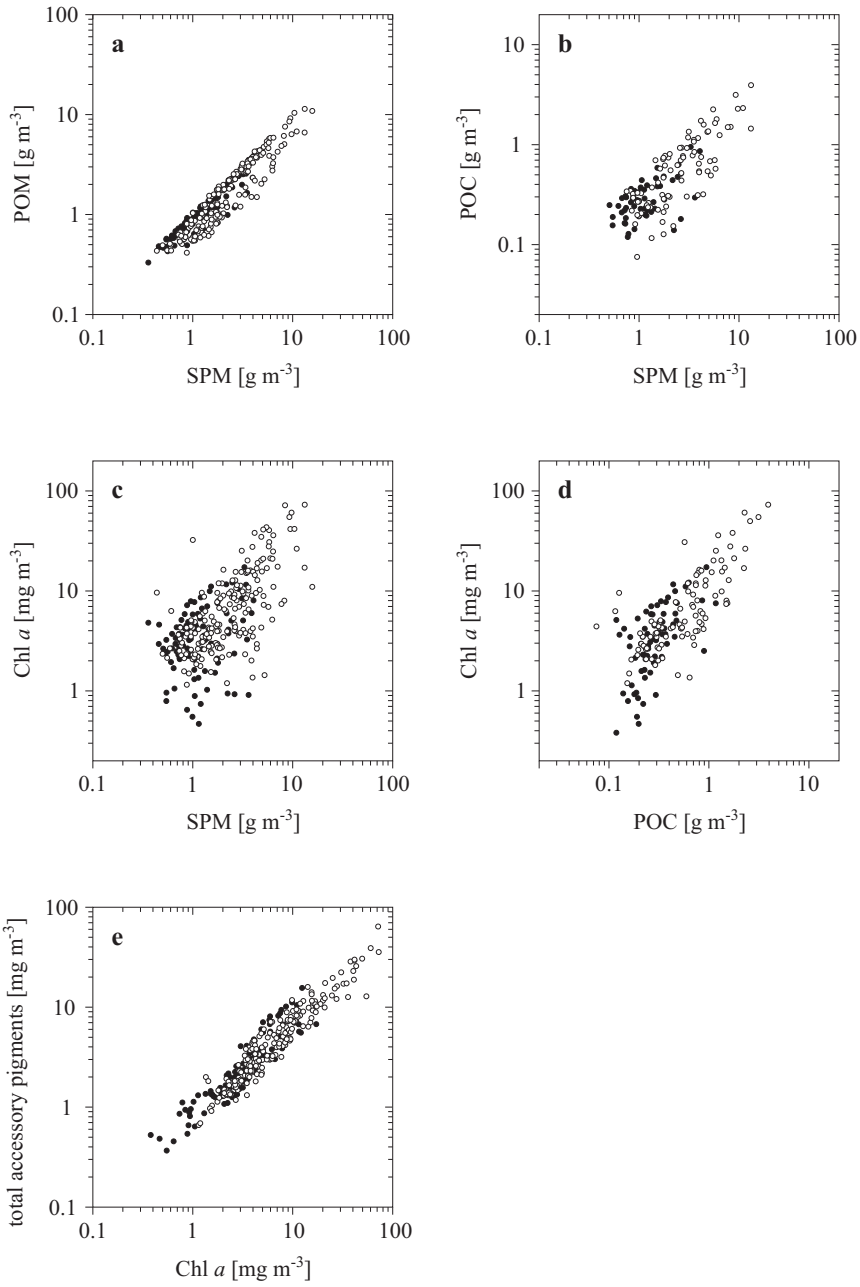

Figure 2. Scatter plots between different biogeochemical parameters: a) POM and SPM; b) POC and SPM; c) Chl *a* and SPM; d) Chl *a* and POC; e) total accessory pigments and Chl *a*. Dark dots – samples from the open waters of the southern Baltic Sea; black circles – samples from the Gulf of Gdańsk

(with the aid of the colour coded data points – see Figure caption for details) that, on average, lower suspended matter concentrations were typical of the open southern Baltic waters rather than of the Gulf of Gdańsk.

The high variability in different concentration measures of particulate matter in southern Baltic waters had to yield a high variability in IOPs. Relationships between particle concentrations and optical properties will be described in detail below, but at this point it is appropriate to emphasize the general variability ranges in particle IOPs. The absorption coefficient of particles at 440 nm varied between < 0.07 m^{-1} and > 3 m^{-1}, an almost 50-fold range (see Table 1). The absorption coefficient separated into the absorption coefficient of phytoplankton pigments $a_p(440)$ and of detritus $a_d(440)$ varied between values below the level of detection and 3 m^{-1} and 1.3 m^{-1} respectively. In addition, different particle scattering characteristics varied significantly: the particle scattering coefficient at 555 nm by > 40 -fold (values up to 9.3 m^{-1}), and the backscattering coefficient at 420 nm by almost 70-fold (values up to 0.23 m^{-1}).

3.2. Light absorption by suspended particulate matter

Before we enter into a detailed description of particulate absorption coefficients it is worth showing the relative proportions between the absorption coefficients of particles and CDOM. Figure 3 shows the absorption budget for the non-water constituents of seawater (there, absorption is separated into components a_d, a_{ph} and a_{CDOM}). As can be seen, the absorption of non-water constituents in all our samples is dominated by CDOM at short wavelengths of light. At 350 nm and 400 nm the respective average contributions of particles $(a_{ph} + a_d)$ to the total non-water absorption $(a_{ph} + a_d + a_{\mathrm{CDOM}})$ are ca 12% and 27%. But with increasing wavelengths the average contribution of particles increases to significant and even dominant values: it is ca 45% at 440 nm, ca 56% at 500 nm and ca 75% at 600 nm. These contributions in individual samples also exhibit a large variability in their proportions at longer wavelengths.

In this paper we focus on analyses of the variability of constituent-specific IOPs. These are optical coefficients normalized to the concentrations of certain seawater constituents. Such average values are often sought as they provide an easy way of describing the connections between biogeochemical and optical quantities. Below we show that such average values in the southern Baltic are unfortunately encumbered with a very high variability.

Figures 4 and 5, and Table 2, present a summary of the results of the variability analysis of constituent-specific absorption coefficients. Figure 4a shows spectra of the mass-specific coefficient of particles $a_p{}^*(\lambda)$

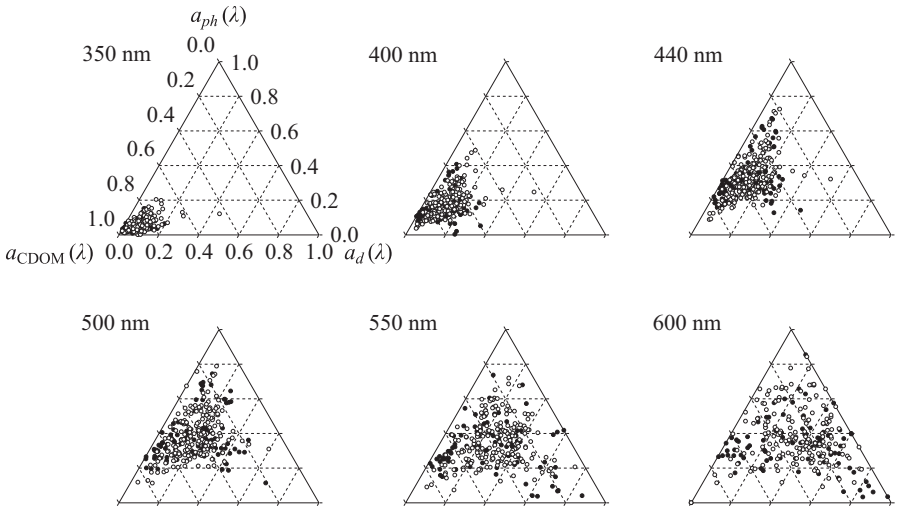

Figure 3. Ternary plots presenting the relative contribution of CDOM, detritus and phytoplankton pigments to total absorption by non-water constituents at different wavelengths. The relative contribution of a given component was calculated as the ratio of the absorption coefficient of that component (e.g. a_{CDOM}) to the sum of the absorption coefficients of all three components ($a_{\mathrm{CDOM}} + a_d + a_{ph}$). The higher the relative contribution of a sample, the closer the data point is to the corresponding triangle apex. The data points are colour coded as in Figure 2

(i.e. the coefficient obtained by normalizing $a_p(\lambda)$ to SPM). Comparison of all the individual sample spectra indicates a large variability of $a_p{}^*$ at all wavelengths. Average values of $a_p{}^*$ and their corresponding standard deviations (SD) and coefficient of variations (CV) for seven wavelengths, chosen to cover the whole measured spectrum, are given in the first row of Table 2. Of these seven wavelengths the 440 and 550 nm bands are the ones where the variability is smallest (but still significant); the corresponding CV is 71% (the average $a_p{}^*$ at 440 nm is 0.198 $\mathrm{m^2\ g^{-1}}$ and at 550 nm is about 0.065 $\mathrm{m^2\ g^{-1}}$). Throughout the rest of the spectrum, the variability described in terms of CV values is even higher – up to 81%. By way of example, a 440 nm band representing the lowest $a_p{}^*(\lambda)$ variability is presented graphically in Figure 5a, in which the relationship between $a_p(440)$ and SPM is plotted for all our samples. The simple linear relation based on the calculated average value of $a_p{}^*$ is shown by a thin solid line. Average values $a_p{}^* \pm \mathrm{SD}$ are plotted for the reference (the two thin dashed lines). We also calculated the best-fit power function between $a_p(440)$ and SPM. The equation coefficients and statistical parameters describing the quality of this fit are given in the first row of Table 3. The fit itself is also plotted in Figure 5a as a thick solid line: this best-fit power function shows that

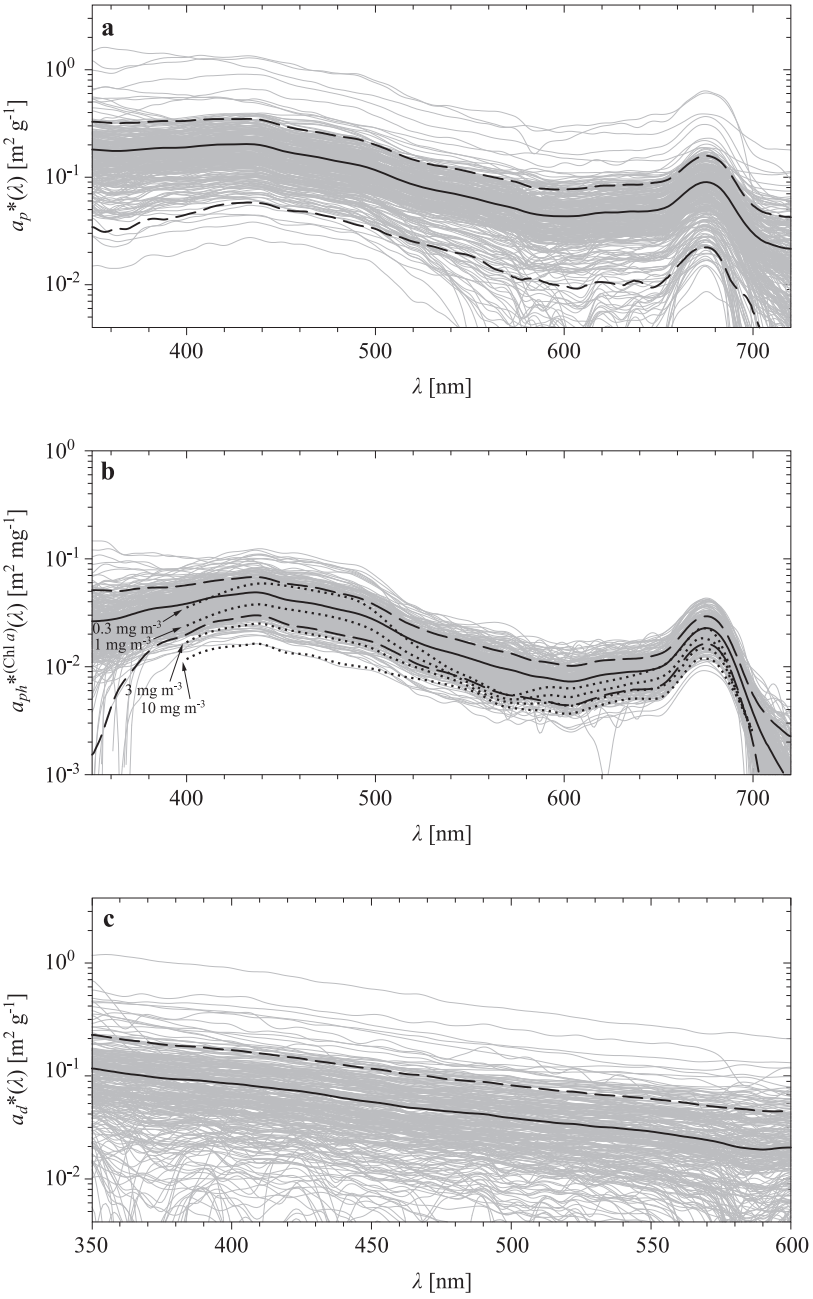

Figure 4. Spectra of a) the mass-specific absorption coefficient of particles $a_p{}^*(\lambda)$; and b) the Chl *a*-specific absorption coefficient of phytoplankton pigments $a_{ph}{}^{*(\mathrm{Chl}\ a)}(\lambda)$; c) the mass-specific absorption coefficient of detritus $a_d{}^*(\lambda)$ for all our southern Baltic Sea samples (shown as thin grey lines). In each panel the corresponding ave- (*continued on next page*)

(**Figure 4**, *continued*) rage spectrum is given by a solid black line and the range of average ± SD by dashed black lines. Small-scale irregularities in the spectra represent measurement noise. Additionally, in panel b, the dotted lines represent four different example spectra of ${a_{ph}}^{*(\text{Chl } a)}$ for oceanic waters according to Bricaud et al. (1998) (calculated for values of Chl a of 0.3, 1, 3 and 10 mg m^{-3})

there is a deviation from linearity in the relation between $a_p(440)$ and SPM (as the power in the fit equation is 0.703, which is much less than 1).

If the particle absorption coefficient $a_p(\lambda)$ is normalized to Chl a (giving the chlorophyll-specific absorption coefficients of particles ${a_p}^{*(\text{Chl } a)}(\lambda)$), the corresponding variability is smaller at some wavelengths (400, 440 and 500 nm) and higher at others (350, 550, 600 and 675 nm) when compared to the variability in ${a_p}^*(\lambda)$ (see the data in the second row of Table 2). In the case of the chlorophyll-specific coefficient, the 440 nm band also has the smallest variability across the whole spectrum, and the corresponding CV value is 59% (which is smaller than in the case of ${a_p}^*(440)$). The relation between $a_p(440)$ and Chl a is presented in Figure 5b. The average value of $a_p^{*(\text{Chl } a)}(440)$ is about 0.073 m^2 mg^{-1}. For the best power function fit we get an equation of $a_p(440) = 0.104\ (\text{Chl } a)^{0.690}$ (plotted as a thick solid line in Figure 5b; the statistical parameters of the equation are given in Table 3), which indicates a significant deviation from linearity in the relation between $a_p(440)$ and Chl a. This particular best-fit equation is directly comparable with the similar average equation, obtained by Bricaud et al. (1998), describing the coefficient of light absorption by suspended particles in oceanic (case I) waters as a function of Chl a: $a_p(440) = 0.052\ (\text{Chl } a)^{0.635}$ (for reference, shown as a thick dashed line in Figure 5b). As can be seen, our results obtained for southern Baltic waters suggest that the average efficiency of absorption by suspended particles measured per unit of Chl a is about twice as high as the average absorption for oceanic particles reported by Bricaud et al. (1998). At this point, let us stress that in theory such a difference in particle absorption properties may be generated by differences in both particle size distributions (PSDs) (influencing the so-called package effect) and the composition of suspended matter (of both pigmented and non-pigmented matter) (see e.g. Morel & Bricaud 1981, Bohren & Huffman 1983, Jonasz & Fournier 2007). Regardless of the fact that we estimated different major biogeochemical parameters characterizing populations of suspended particles, in our series of field experiments we were unfortunately not able to measure PSDs (to be precise, Bricaud et al. (1998) did not provide size distribution data in their work either). As PSDs cannot be directly compared, we can only confront our results with those from the

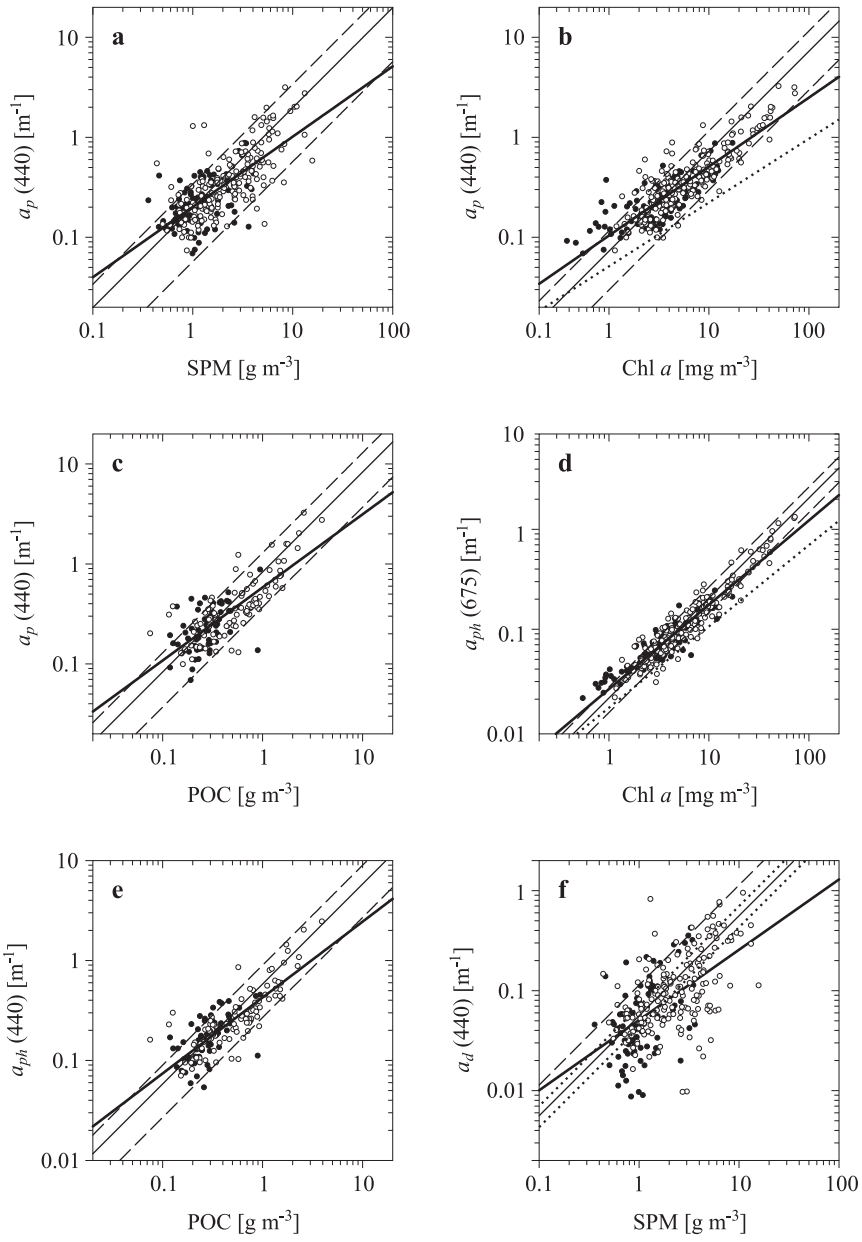

Figure 5. Relationships between a) the absorption coefficient of particles $a_p(440)$ and SPM; b) $a_p(440)$ and Chl a; c) $a_p(440)$ and POC; d) the absorption coefficient of phytoplankton pigments $a_{ph}(675)$ and Chl a; e) $a_{ph}(440)$ and POC; and f) the absorption coefficient of detritus, $a_d(440)$, and SPM. The data points are colour coded as in Figure 2. The thin solid lines represent linear relations (passing through the origin) based on the average values of the constituent specific absorption coefficients (see also Table 2), the thin (*continued on next page*)

(**Figure 5**, *continued*) dashed lines represent the ranges of average ± SD, and the thick lines represent the best-fit power functions (see also Table 4, p. 716). Additionally, in panels b and d, dotted lines are plotted representing two equations obtained for oceanic (case I) waters according to Bricaud et al. (1998) (the equations $a_p(440) = 0.052$ (Chl a)$^{0.635}$ and $a_{ph}(674) = 0.0182$ (Chl a)$^{0.813}$ respectively); in panel f two dotted lines represent average values of $a_d{}^*(440)$ calculated according to Babin et al. (2003b) (the upper curve stands for the equation $a_d{}^*(440) = 0.070$ m^2 g^{-1} for their Baltic samples and the lower curve stands for the equation $a_d{}^*(440) = 0.043$ m^2 g^{-1} for all their samples from different coastal waters around Europe)

literature, but without giving a full physical explanation of differences: we can merely speculate. We are also aware that in practice we cannot rule out the possibility that at least the part of the observed differences may be caused by unwanted methodological inaccuracies related, e.g. to the estimation of particle absorption coefficient spectra, which involves the use of a β-factor correction for filter pad technique measurements (see e.g. the extensive discussion on the β-factor in Bricaud & Stramski (1990)). Here, we can only state that in our work we applied the β-factor according to Kaczmarek et al. (2003) which, to our knowledge, should be best suited to the correction of absorption coefficient measurements performed in different coastal waters.

Our average $a_p{}^{*(\text{Chl } a)}$ results can also be compared with the handful of values reported in the literature for case II waters. For a selected group of their samples from Irish Sea shelf waters (samples with a relatively high Chl a/SPM concentration ratio) McKee & Cunningham (2006) reported average values of $a_p{}^{*(\text{Chl } a)}(440) = 0.054$ m^2 mg^{-1} (± 0.007 m^2 mg^{-1}) and $a_p{}^{*(\text{Chl } a)}(676) = 0.022$ m^2 mg^{-1} (± 0.003 m^2 mg^{-1}). Our averaged southern Baltic values are about 35–45% higher than those of McKee & Cunningham (2006), but also exhibit a higher variability (recall that for our data we obtained average values of about 0.073 m^2 mg^{-1} (± 0.043 m^2 mg^{-1}) and 0.032 m^2 mg^{-1} (± 0.022 m^2 mg^{-1}) for wavelengths 440 nm and 675 nm respectively).

As in the case of SPM and Chl a, the values of $a_p(\lambda)$ can also be normalized to POC and POM. Examples of spectral average values and the variability of POC-specific and POM-specific particle absorption coefficients ($a_p^{*(\text{POC})}(\lambda)$ and $a_p{}^{*(\text{POM})}(\lambda)$) are given in the third and fourth rows of Table 2. Across all wavelengths the variability of $a_p{}^{*(\text{POC})}(\lambda)$ described in terms of CV turns out to be smaller than the variability of chlorophyll-specific a_p. Nonetheless, it should be noted that the number of samples taken into account in the analyses of POC – a_p relationships is about two times smaller than in the previous cases, which may to some extent

Table 2. Variability of constituent-specific absorption coefficients of particles, constituent-specific absorption coefficients of phytoplankton pigments, and constituent-specific absorption coefficients of detritus. For each constituent-specific coefficient the average value, standard deviation (in italics), and coefficient of variation (in parentheses) are given

Constituent-specific coefficient	Light wavelength (λ)							Number of samples
	350 nm	400 nm	440 nm	500 nm	550 nm	600 nm	675 nm	
$a_p{}^*(\lambda)$	1.81E-01	1.90E-01	**1.98E-01**	1.16E-01	**6.51E-02**	4.32E-02	9.02E-02	
[m^2 g^{-1}]	*1.47E-01*	*1.45E-01*	*1.41E-01*	*8.32E-02*	*4.64E-02*	*3.37E-02*	*6.80E-02*	285
	(81%)	(76%)	**(71%)**	(72%)	**(71%)**	(78%)	(75%)	
$a_p{}^{*(\mathrm{Chl\ a})}(\lambda)$	7.18E-02	7.06E-02	**7.27E-02**	4.32E-02	2.42E-02	1.70E-02	3.18E-02	
[m^2 mg^{-1}]	*6.93E-02*	*4.95E-02*	*4.30E-02*	*2.86E-02*	*2.07E-02*	*1.89E-02*	*2.18E-02*	323
	(97%)	(70%)	**(59%)**	(66%)	(85%)	(111%)	(68%)	
$a_p{}^{*(\mathrm{POC})}(\lambda)$	7.58E-01	7.84E-01	**8.32E-01**	4.95E-01	2.78E-01	1.87E-01	3.71E-01	
[m^2 g^{-1}]	6.09E-01	4.94E-01	4.62E-01	2.83E-01	1.99E-01	1.68E-01	2.36E-01	163
	(80%)	(63%)	**(55%)**	(57%)	(72%)	(90%)	(64%)	
$a_p{}^{*(\mathrm{POM})}(\lambda)$	2.53E-01	2.56E-01	**2.60E-01**	**1.53E-01**	8.74E-02	5.89E-02	**1.17E-01**	
[m^2 g^{-1}]	*2.60E-01*	*2.25E-01*	*1.90E-01*	*1.12E-01*	*6.79E-02*	*5.28E-02*	*8.58E-02*	273
	(103%)	(88%)	**(73%)**	**(73%)**	(78%)	(90%)	**(73%)**	
$a_{ph}{}^*(\lambda)$	7.60E-02	1.14E-01	**1.43E-01**	7.98E-02	3.77E-02	2.34E-02	7.30E-02	
[m^2 g^{-1}]	*7.17E-02*	*8.52E-02*	*1.06E-01*	*6.09E-02*	*2.89E-02*	*2.18E-02*	*6.25E-02*	277
	(94%)	(75%)	**(74%)**	(76%)	(77%)	(93%)	(86%)	

Table 2. (*continued*)

Constituent-specific coefficient	Light wavelength (λ)							Number of samples
	350 nm	400 nm	440 nm	500 nm	550 nm	600 nm	675 nm	
${a_{ph}}^{*(\text{Chl } a)}(\lambda)$	2.63E-02	3.84E-02	4.82E-02	2.68E-02	1.19E-02	7.34E-03	**2.28E-02**	
[m^2 mg^{-1}]	*2.48E-02*	*1.85E-02*	*1.87E-02*	*1.02E-02*	*4.54E-03*	*2.94E-03*	*6.51E-03*	312
	(94%)	(48%)	(39%)	(38%)	(38%)	(40%)	**(29%)**	
${a_{ph}}^{*(\text{POC})}(\lambda)$	2.69E-01	4.52E-01	**5.83E-01**	**3.26E-01**	1.48E-01	8.84E-02	2.82E-01	
[m^2 g^{-1}]	*3.28E-01*	*2.75E-01*	*3.14E-01*	*1.75E-01*	*9.81E-02*	*5.21E-02*	*1.67E-01*	159
	(122%)	(61%)	**(54%)**	**(54%)**	(66%)	(59%)	(59%)	
${a_{ph}}^{*(\text{POM})}(\lambda)$	1.03E-01	1.49E-01	**1.82E-01**	**1.01E-01**	4.79E-02	3.00E-02	9.20E-02	
[m^2 g^{-1}]	*9.69E-02*	*1.04E-01*	*1.16E-01*	*6.52E-02*	*3.13E-02*	*2.40E-02*	*6.80E-02*	265
	(94%)	(70%)	**(64%)**	**(64%)**	(65%)	(80%)	(74%)	
${a_d}^*(\lambda)$	1.05E-01	7.62E-02	5.60E-02	3.67E-02	2.75E-02	1.95E-02	1.75E-02	
[m^2 g^{-1}]	*1.10E-01*	*7.95E-02*	*5.75E-02*	*3.66E-02*	*2.75E-02*	*2.28E-02*	*2.19E-02*	277
	(105%)	(104%)	(103%)	(100%)	(100%)	(117%)	(125%)	
${a_d}^{*(\text{POC})}(\lambda)$	4.97E-01	3.37E-01	2.53E-01	1.73E-01	1.33E-01	9.94E-02	9.23E-02	
[m^2 g^{-1}]	*5.65E-01*	*3.17E-01*	*2.52E-01*	*1.91E-01*	*1.69E-01*	*1.60E-01*	*1.60E-01*	159
	(114%)	(94%)	(99%)	(111%)	(128%)	(161%)	(173%)	

Table 3. Examples of best-fit power functions ($y = C_1 x^{C_2}$) between absorption coefficients of particles, absorption coefficients of phytoplankton pigments, absorption coefficients of detritus and concentrations of certain constituents. The r^2 value between the log-transformed data, mean normalized bias (MNB*), normalized root mean square error (NRMSE**), and number of samples (n), are also given for each fitted function

Relationship	C_1	C_2	r^2	MNB [%]	NRMSE [%]	n
$a_p(440)$ vs. SPM	2.01×10^{-1}	7.03×10^{-1}	0.53	12.4	58.1	285
$a_p(440)$ vs. Chl a	1.04×10^{-1}	6.90×10^{-1}	**0.73**	**6.4**	**36.6**	323
$a_p(440)$ vs. POC	5.83×10^{-1}	7.31×10^{-1}	0.62	9.2	48.4	163
$a_p(440)$ vs. POM	2.42×10^{-1}	7.12×10^{-1}	0.54	12.6	58.8	273
$a_{ph}(440)$ vs. SPM	1.44×10^{-1}	6.86×10^{-1}	0.51	13.1	59.1	277
$a_{ph}(440)$ vs. Chl a	6.55×10^{-2}	7.63×10^{-1}	0.83	4.4	31.6	312
$a_{ph}(675)$ vs. Chl a	2.80×10^{-2}	8.43×10^{-1}	**0.90**	**3.0**	**25.6**	312
$a_{ph}(440)$ vs. POC	4.26×10^{-1}	7.59×10^{-1}	0.66	8.1	45.5	159
$a_{ph}(440)$ vs. POM	1.71×10^{-1}	7.44×10^{-1}	0.59	11.4	56.3	265
$a_d(440)$ vs. SPM	5.08×10^{-2}	7.03×10^{-1}	0.32	41.8	170.3	265
$a_d(500)$ vs. SPM	3.56×10^{-2}	6.87×10^{-1}	0.32	36.1	134.5	254
$a_d(400)$ vs. POC	1.77×10^{-1}	6.44×10^{-1}	0.25	49.7	129.2	156

* $\mathrm{MNB} = \frac{1}{\mathrm{n}} \sum_{i=1}^{\mathrm{n}} \left(\frac{P_i - O_i}{O_i} \right) \times 100$, where P_i – predicted value, O_i – measured value;

** $\mathrm{NRMSE} = \left[\frac{1}{\mathrm{n}-1} \sum_{i=1}^{\mathrm{n}} \left(\frac{P_i - O_i}{O_i} - \frac{\mathrm{MNB}}{100} \right)^2 \right]^{\frac{1}{2}} \times 100$.

affect the corresponding values of SD and CV. 440 nm is again the best light wavelength with which to linearly relate a_p to POC. For the average ${a_p}^{*(\mathrm{POC})}(440)$ (equal to about 0.83 $\mathrm{m^2\ g^{-1}}$) the corresponding CV is 55%. The relation between $a_p(440)$ and POC is presented in Figure 5c, and the best-fit power equation in Table 3. The variability of ${a_p}^{*(\mathrm{POM})}$ is relatively high (at almost all wavelengths it is higher than that of ${a_p}^*$), with the smallest values of CV (73%) obtained at 440, 500 and 675 nm. An example of a best-fit power equation between $a_p(440)$ and POM is given in Table 3.

All the above results refer to absorption coefficients of (all) particles and how they may be related to SPM, Chl a, POC and POM. The next step is a similar analysis of the absorption coefficient of phytoplankton pigments $a_{ph}(\lambda)$. Figure 4b shows the spectra of the chlorophyll-specific coefficient ${a_{ph}}^{*(\mathrm{Chl\ }a)}(\lambda)$ for all the samples recorded as well as the average value, and the average $\pm$ SD. The variability in average ${a_{ph}}^{*(\mathrm{Chl\ }a)}$ across all wavelengths lies within the CV range from about 29% to 94% (see

also row 6 of Table 2). The smallest values of CV (29%) is reached at 675 nm, i.e. in the vicinity of the 'red' peak of absorption by phytoplankton pigments (the respective average value of $a_{ph}{}^{*(\text{Chl } a)}(675)$ is 0.0228 m^2 mg^{-1}). Throughout the range of light wavelengths between 440 and 600 nm, CV values also remain relatively small (not exceeding 40%). The presented average $a_{ph}{}^{*(\text{Chl } a)}$ spectra can be compared with the average spectra reported for oceanic waters by Bricaud et al. (1998) (see the dotted lines in Figure 4b representing different $a_{ph}{}^{*(\text{Chl } a)}$ spectra calculated for four different values of Chl a – 0.3, 1, 3 and 10 mg m^{-3}). Our average $a_{ph}{}^{*(\text{Chl } a)}$ spectrum is similar in shape to the two given by Bricaud et al. (1998) for Chl a values of 3 and 10 mg m^{-3}, but regardless of this similarity, the absolute values of our average spectrum are distinctively higher (we recall that in our study, the values of Chl a changed over a range from less than 0.4 to more than 70 mg m^{-3} with an average value of about 7.6 mg m^{-3}). Examples of best-fit power functions between $a_{ph}(440)$ and Chl a, and $a_{ph}(675)$ and Chl a, found for our Baltic data are given in Table 3. The relationship between $a_{ph}(675)$ and Chl a is also plotted in Figure 5d. Compared with the similar power function fit of a_{ph} vs. Chl a for oceanic waters reported by Bricaud et al. (1998) (see the dotted line in Figure 5d representing the equation for the adjacent wavelength of 674 nm: $a_{ph}(674) = 0.0182(\text{Chl } a)^{0.813}$), the power function fit obtained in the present work shows a similar value of the power, but the value of the constant C_1 is about 50% higher. This again suggests that on average the efficiency of light absorption (this time absorption by phytoplankton pigments alone) per unit of chlorophyll a in our southern Baltic Sea samples is higher when compared with average oceanic results. As we said earlier, since we cannot directly compare PSDs for our Baltic samples with the size distributions for oceanic samples reported by Bricaud et al. (1998), we can only speculate about the reasons for such differences in the chlorophyll-specific absorption coefficient. Interestingly, Babin et al. (2003b) reported a qualitatively similar feature – distinctively higher $a_{ph}{}^{*(\text{Chl } a)}$ values for at least for some parts of the visible light spectrum for their Baltic Sea samples compared with averaged oceanic results (see the spectrum and spread of data points representing Baltic samples in their original Figures 6c and 7). Unfortunately, apart from these figures, Babin et al. (2003b) presented no explicit $a_{ph}{}^{*(\text{Chl } a)}$ statistics for Baltic samples, so we cannot compare these results quantitatively. However, our average values of $a_{ph}{}^{*(\text{Chl } a)}(440)$ can be directly compared with other data given by Vantrepotte et al. (2007) for the eastern English Channel. These authors reported an average $a_{ph}{}^{*(\text{Chl } a)}(440)$ value of about 0.048 m^2 mg^{-1} ($\pm$ 0.024 m^2 mg^{-1}) for their winter samples,

which is very similar to our average value (recall that we obtained a value of about 0.048 $m^2\ mg^{-1} \pm 0.019\ m^2\ mg^{-1}$), but at the same time they also gave an approximately threefold lower average value for their spring and summer samples – a value of 0.018 $m^2\ mg^{-1}$ ($\pm 0.004\ m^2\ mg^{-1}$). The spread of our results for the red part of the spectrum (our average ${a_{ph}}^{*(\text{Chl } a)}(675)$ is 0.023 $m^2\ mg^{-1} \pm 0.007\ m^2\ mg^{-1}$) also seems to be at least partially convergent with the results presented by Oubelkheir et al. (2006) for the tropical coastal waters off eastern Australia. They reported on a wide range of possible ${a_{ph}}^{*(\text{Chl } a)}(676)$ values between 0.008 and 0.030 $m^2\ mg^{-1}$. Interestingly, a common factor in all the papers cited above is that all authors, regardless of the differences in average values they present, report a significant variability in the values of ${a_{ph}}^{*(\text{Chl } a)}$ for coastal (case II) waters.

Table 2 (rows 5, 7 and 8) also presents average values and variability of $a_{ph}(\lambda)$ normalized to SPM, POC and POM. At the seven light wavelengths selected and for almost all comparable cases the variability of ${a_{ph}}^*(\lambda)$, ${a_{ph}}^{*(\text{POC})}$ and ${a_{ph}}^{*(\text{POM})}$ is higher than it was in the case of ${a_p}^{*(\text{Chl } a)}$. At 440 nm CV reaches its lowest values for each constituent-specific coefficient – 74%, 54% and 64% for ${a_{ph}}^*(440)$, ${a_{ph}}^{*(\text{POC})}(440)$ and ${a_{ph}}^{*(\text{POM})}(440)$ respectively. The relationship between $a_{ph}(440)$ and POC is plotted in Figure 5e, and the best-fit equations between $a_{ph}(440)$ and SPM, POC or POM, are also given in Table 3.

Finally, we mention the results concerning the absorption of light by detritus. Before we present the resultant constituent-specific absorption coefficients of detritus, let us briefly characterize the shapes of the a_d spectra that we obtained for our Baltic samples. Once all the spectra had been fitted with an exponential function ($a_d(\lambda) = C_1 \exp[-S_d(\lambda - \lambda_{\text{ref}})]$), we found the average slope S_d to be 0.0070 nm^{-1} ($\pm 0.0027\ nm^{-1}$) (fitting was performed for a range of wavelengths between 350 and 600 nm). Compared with the literature values given by Babin et al. (2003b) (they found the average spectral slope S_d to be 0.0130 nm^{-1} ($\pm 0.0007\ nm^{-1}$) for their Baltic samples and 0.0123 nm^{-1} ($\pm 0.0013\ m^{-1}$) for all their coastal samples), our value seems to be distinctly lower (and as a result our average spectrum seems to be flatter). But at this point it is important to note that Babin et al. (2003b) had all their a_p and a_d spectra corrected to show no absorption at the wavelength of 750 nm. For our data we chose a different methodological approach: we corrected our a_d spectra in order to have the same value as the a_p spectra at wavelength 750 nm, but at the same time our a_p spectra were not forced to reach zero in the infrared (as we believe the a_p spectra obtained with Transmission-Reflectance (T-R) algorithm (Tassan & Ferrari 1995, 2002) should not require such a correction). If we had applied the same

type of a_d spectra correction as Babin et al. (2003b) did, we would have obtained a different average value of S_d – 0.0098 nm^{-1} ($\pm$ 0.0028 nm^{-1}). This last value is still smaller but closer to the values reported by Babin et al. (2003b). Such a hypothetical average S_d would also be comparable to the values reported by Bricaud et al. (1998) for their oceanic samples (note that Bricaud et al. in their work also forced a_d spectra to reach zero at 750 nm). These authors estimated the average S_d to be 0.0110 nm^{-1} ($\pm$ 0.0020 nm^{-1}) when they took into account all their data and also an average value of 0.0100 nm^{-1} ($\pm$ 0.0010 nm^{-1}) for the group of samples with Chl *a* restricted to the range between 1 and 10 mg m^{-3}.

Figure 4c shows the spectra of the mass-specific absorption coefficients of detritus $a_d{}^*(\lambda)$ for all samples recorded as well as the average spectrum and range of its SD. The variability in this case is distinctly greater than the variability of $a_p{}^*$ presented earlier. Examples of average $a_d{}^*$ values and the corresponding CVs can be found in row 9 of Table 2. Those CV values lie between 100% and 125%, which indicates that the relationships between $a_d(\lambda)$ and SPM are weak in the case of our data; this is also illustrated by the spread of the data points ($a_d(440)$ vs. SPM) in Figure 5f. Additionally, for comparison, in Figure 5f we also present two curves plotted according to the results of Babin et al. (2003b). They reported an average value of $a_d{}^*(443)$ of 0.067 m^2 g^{-1} ($\pm$ 0.022 m^2 g^{-1}) for their Baltic samples and an average $a_d{}^*(443)$ value of 0.041 m^2 g^{-1} ($\pm$ 0.023 m^2 g^{-1}) for all their samples from coastal waters around Europe. These cited average $a_d{}^*$ values converted to wavelength 440 nm (with the help of the already-mentioned average slopes of a_d spectra) would reach values of 0.070 and 0.043 m^2 g^{-1} for Baltic and all coastal samples respectively. Our average $a_d{}^*(440)$ value for southern Baltic samples (0.056 m^2 g^{-1}) lies between those two values, but the variability in the case of our samples is much higher (SD = 0.058 m^2 g^{-1}) (note here, too, that the differences in the infrared signal correction should only have a minor influence on the magnitude of a_d at 440 nm). In the case of the absorption coefficient of detritus normalized to POC (see the values in the last row of Table 2) and also normalized to Chl *a* and POM (not shown), the variability is even greater than the variability of $a_d{}^*(\lambda)$. Moreover, the statistical parameters describing the best power function fits between a_d and SPM, and a_d and POC give values much worse than those presented earlier for the relationships between a_p or a_{ph} and SPM, Chl *a*, POC, or POM (compare the values of r^2, the mean normalized bias (MNB) and the normalized root mean square error (NRMSE) given in Table 3). Such a manifest variability of different constituent-specific absorption coefficients of detritus leads us to believe that our own results concerning the estimation of the non-phytoplankton component of absorption should be treated with caution. As

some of us have already experienced during other experiments performed in a different marine environment (see Woźniak et al. 2010), we are aware that partitioning a_p into a_{ph} and a_d by the bleaching technique may sometimes fail to provide reasonable results. On account of the registered ${a_d}^*$ variability (and also for other practical reasons) when, later in this paper, we attempt to find practically useful formulas for the rough estimation of certain seawater constituent concentrations based on measured values of seawater IOPs, we will use values of a_p rather than the results partitioned into a_d and a_{ph}.

3.3. Scattering by suspended particulate matter

Figure 6a shows spectra of the mass-specific scattering coefficient of suspended particles ${b_p}^*(\lambda)$ (i.e. $b_p(\lambda)$ normalized to SPM). The average values (represented in the figure by circles connected by a thick solid line) are also reported in the first row of Table 4, together with corresponding values of SD and CV. This shows that the average spectrum of ${b_p}^*(\lambda)$ is relatively flat. If the particle scattering coefficients $b_p(\lambda)$ are fitted with the power function of const $\times \lambda^{\eta}$ (within the spectral range of all available data, i.e. between 412 and 715 nm), the average spectral slope of scattering η is equal to -0.404 (± 0.432(SD)). The minimum and maximum values of η are -1.3 and 0.779 respectively. It is worth noting that the variability in ${b_p}^*(\lambda)$ is quite similar at all the light wavelengths. All the average spectral values lay between 0.55 and 0.69 $\mathrm{m^2\ g^{-1}}$, and the corresponding values of CV were between 46 and 49% (minimum CV at 650 nm). Among other things, Table 5 lists the best-fit power functions between $b_p(650)$ and SPM, but we also found that the power function fitted between $b_p(555)$ and SPM gives slightly better statistical parameters (lower values of MNB and NRMSE, whereas $\mathrm{r^2}$ remains at the same level (0.73)). This last power function fit line is shown against the background of $b_p(555)$ vs. SPM data points in Figure 7a.

We also calculated average values of $b_p(\lambda)$ normalized to Chl a, POC and POM. Average chlorophyll-specific scattering coefficients ${b_p}^{*(\mathrm{Chl\ }a)}(\lambda)$ are listed in the second row of Table 4. While the average values of ${b_p}^{*(\mathrm{Chl\ }a)}(\lambda)$ are of the order of 2.3–2.9 $\mathrm{m^2\ mg^{-1}}$, their variability is much higher than the variability of ${b_p}^*(\lambda)$ discussed above. At most wavelengths the CV for ${b_p}^{*(\mathrm{Chl\ }a)}(\lambda)$ is $>74\%$ and only at 715 nm does it fall to a minimum of 65%. Average values of the POC-specific particle scattering coefficient ${b_p}^{*(\mathrm{POC})}(\lambda)$ (see third row in Table 4) lie between 2.4 and 3.0 $\mathrm{m^2\ g^{-1}}$, whereas CV variability resembles the variability of ${b_p}^*(\lambda)$. It is smallest at 676 nm (where CV = 46%). The spread of $b_p(676)$ vs. POC data points is presented in Figure 7b, together with the best-fit power function line (see Table 5

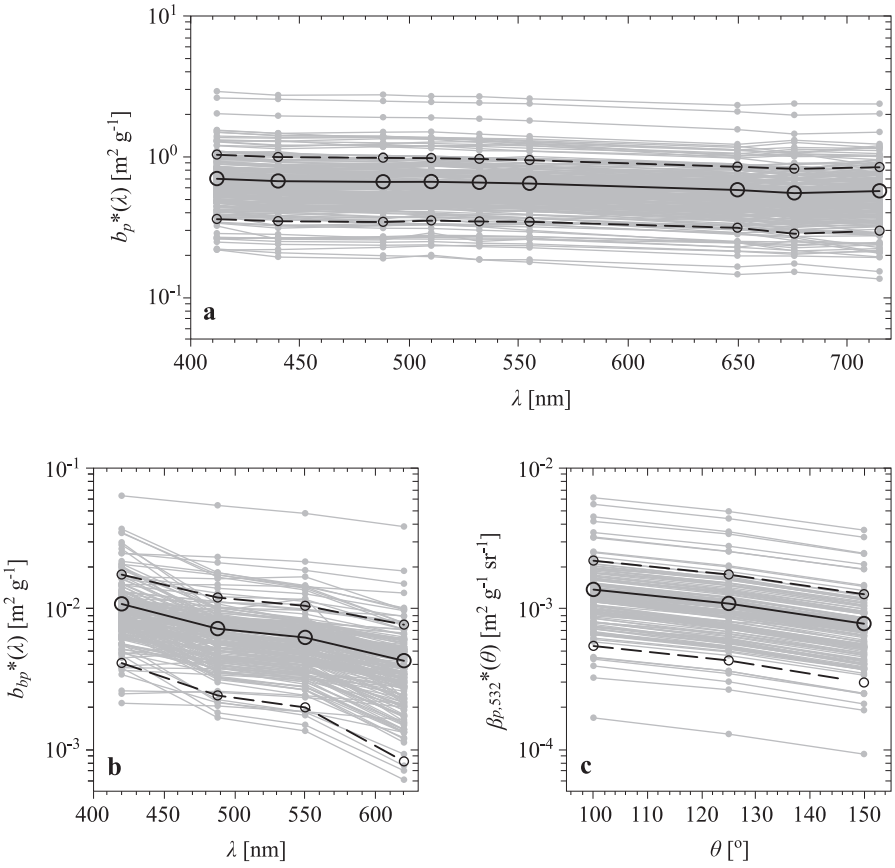

Figure 6. a) Spectra of the mass-specific scattering coefficient of particles $b_p{}^*(\lambda)$; b) spectra of the mass-specific backscattering coefficient of particles $b_{bp}{}^*(\lambda)$; c) the mass-specific particle volume scattering function $\beta_{p,\,532}{}^*(\theta)$ for all samples (shown by small grey points connected by thin grey lines). In each panel the corresponding average constituent-specific coefficients of all samples are shown by large black circles connected by solid black lines and the range of average ± SD by small black circles connected by dashed black lines

for the equation parameters). Average values of the POM-specific particle scattering coefficient $b_p{}^{*(\mathrm{POM})}(\lambda)$ for different wavelengths lie between 6.9 and 8.8 m^2 g^{-1}. The variability is rather similar at all wavelengths, but smallest at 650 nm (CV = 55%). The best-fit power function for that relation is given in the fifth row of Table 5.

Figure 6b illustrates spectral values of the mass-specific backscattering coefficient $b_{bp}{}^*(\lambda)$ (obtained by normalization of $b_{bp}(\lambda)$ values to SPM). If the spectral values of $b_{bp}(\lambda)$ for all samples are fitted with the power function of const $\times\, \lambda^{\eta}$, the average spectral slope η obtained is -2.28 ($\pm$ 1.35

Table 4. Variability of constituent-specific scattering coefficients of particles, constituent-specific backscattering coefficients of particles, and constituent-specific volume scattering functions. For each constituent-specific coefficient the average value, standard deviation (in italics), and coefficient of variation (in parentheses) are given

Constituent-specific coefficient	Light wavelength (λ)									Number of samples
	412 nm	440 nm	488 nm	510 nm	532 nm	555 nm	650 nm	676 nm	715 nm	
$b_p^*(\lambda)$	6.91E-01	6.66E-01	6.57E-01	6.58E-01	6.50E-01	6.40E-01	**5.75E-01**	5.47E-01	5.65E-01	
[m^2 g^{-1}]	*3.34E-01*	*3.21E-01*	*3.17E-01*	*3.11E-01*	*3.07E-01*	*2.98E-01*	*2.66E-01*	*2.67E-01*	*2.71E-01*	223
	(48%)	(48%)	(48%)	(47%)	(47%)	(47%)	**(46%)**	(49%)	(48%)	
$b_p^{*(\text{Chl } a)}(\lambda)$	2.94E-01	2.85E-01	2.76E-01	2.77E-01	2.73E-01	2.70E-01	2.41E-01	2.31E-01	**2.26E-01**	
[m^2 mg^{-1}]	*2.38E-01*	*2.33E-01*	*2.14E-01*	*2.13E-01*	*2.08E-01*	*2.08E-01*	*1.78E-01*	*1.74E-01*	*1.47E-01*	252
	(81%)	(82%)	(77%)	(77%)	(76%)	(77%)	(74%)	(76%)	**(65%)**	
$b_p^{*(\text{POC})}(\lambda)$	3.00E+00	2.92E+00	2.86E+00	2.88E+00	2.85E+00	2.83E+00	2.55E+00	**2.41E+00**	2.44E+00	
[m^2 g^{-1}]	*1.52E+00*	*1.49E+00*	*1.43E+00*	*1.42E+00*	*1.39E+00*	*1.37E+00*	*1.20E+00*	*1.10E+00*	*1.13E+00*	148
	(51%)	(51%)	(50%)	(49%)	(49%)	(49%)	(47%)	**(46%)**	(47%)	
$b_p^{*(\text{POM})}(\lambda)$	8.78E-01	8.46E-01	8.35E-01	8.37E-01	8.25E-01	8.12E-01	**7.30E-01**	6.93E-01	7.15E-01	
[m^2 g^{-1}]	*5.06E-01*	*4.92E-01*	*4.82E-01*	*4.75E-01*	*4.69E-01*	*4.58E-01*	*4.05E-01*	*3.92E-01*	*4.03E-01*	223
	(58%)	(58%)	(58%)	(57%)	(57%)	(56%)	**(55%)**	(57%)	(56%)	

Table 4. (*continued*)

Constituent-specific coefficient	Light wavelength (λ)				Number of samples
	420 nm	488 nm	550 nm	620 nm	
$b_{bp}{}^{*}(\lambda)$	**1.07E-02**	7.15E-03	6.19E-03	4.23E-03	
[m^2 g^{-1}]	*6.66E-03*	*4.76E-03*	*4.22E-03*	*3.42E-03*	196
	(62%)	(67%)	(68%)	(81%)	
$b_{bp}{}^{*(\mathrm{Chl\ a})}(\lambda)$	4.54E-03	2.96E-03	**2.58E-03**	1.81E-03	
[m^2 mg^{-1}]	*4.49E-03*	*2.48E-03*	*2.13E-03*	*1.67E-03*	224
	(99%)	(84%)	**(83%)**	(92%)	
$b_{bp}{}^{*(\mathrm{POC})}(\lambda)$	4.49E-02	3.07E-02	**2.65E-02**	**1.86E-02**	
[m^2 g^{-1}]	*3.70E-02*	*2.23E-02*	***1.85E-02***	*1.29E-02*	135
	(82%)	(73%)	**(70%)**	**(70%)**	
$b_{bp}{}^{*(\mathrm{POM})}(\lambda)$	**1.46E-02**	9.85E-03	8.53E-03	5.91E-03	
[m^2 g^{-1}]	*1.34E-02*	*9.93E-03*	*8.72E-03*	*6.98E-03*	196
	(92%)	(101%)	(102%)	(118%)	

Constituent-specific coefficient	Scattering angle (θ)			Number of samples
	100°	125°	150°	
$\beta_{p,\,532}{}^{*}(\theta)$	1.36E-03	1.08E-03	7.79E-04	
[m^2 g^{-1} sr^{-1}]	*8.23E-04*	*6.58E-04*	*4.83E-04*	151
	(60%)	(61%)	(62%)	
$\beta_{p,\,532}{}^{*(\mathrm{Chl\ a})}(\theta)$	5.89E-04	4.69E-04	3.38E-04	
[m^2 mg^{-1} sr^{-1}]	*6.10E-04*	*4.85E-04*	*3.55E-04*	176
	(104%)	(103%)	(105%)	
$\beta_{p,\,532}{}^{*(\mathrm{POC})}(\theta)$	5.87E-03	4.68E-03	3.37E-03	
[m^2 g^{-1} sr^{-1}]	*5.13E-03*	*4.07E-03*	*3.00E-03*	93
	(87%)	(87%)	(89%)	
$\beta_{p,\,532}{}^{*(\mathrm{POM})}(\theta)$	1.82E-03	1.45E-03	1.04E-03	
[m^2 g^{-1} sr^{-1}]	*1.36E-03*	*1.08E-03*	*7.96E-04*	151
	(74%)	(75%)	(76%)	

Table 5. Examples of best-fit power functions ($y = C_1 x^{C_2}$) between particle scattering coefficients, particle backscattering coefficients, volume scattering functions and concentrations of certain constituents. The r^2 value between the log-transformed data, mean normalized bias (MNB), normalized root mean square error (NRMSE) and number of samples (n) are also given for each fitted function

Relationship	C_1	C_2	r^2	MNB(%)	NRMSE(%)	n
$b_p(650)$ vs. SPM	5.74×10^{-1}	8.52×10^{-1}	**0.73**	8.1	44.8	223
$b_p(555)$ vs. SPM	6.52×10^{-1}	8.15×10^{-1}	**0.73**	7.2	41.7	223
$b_p(715)$ vs. Chl a	3.20×10^{-1}	6.76×10^{-1}	0.64	11.7	55.7	252
$b_p(676)$ vs. POC	1.80	7.54×10^{-1}	0.72	**6.6**	**39.7**	148
$b_p(650)$ vs. POM	6.97×10^{-1}	8.48×10^{-1}	0.72	8.0	43.9	223
$b_{bp}(420)$ vs. SPM	1.01×10^{-2}	9.00×10^{-1}	**0.68**	11.1	54.4	196
$b_{bp}(550)$ vs. Chl a	3.61×10^{-3}	6.44×10^{-1}	0.56	14.9	61.2	224
$b_{bp}(550)$ vs. POC	1.90×10^{-2}	7.81×10^{-1}	0.60	**11.7**	**47.8**	135
$b_{bp}(620)$ vs. POC	1.34×10^{-2}	8.35×10^{-1}	0.56	17.9	69.3	135
$b_{bp}(420)$ vs. POM	1.28×10^{-2}	8.34×10^{-1}	0.60	12.4	49.7	196
$\beta_{p,\,532}(100°)$ vs. SPM	1.41×10^{-3}	7.71×10^{-1}	**0.63**	11.1	55.7	151
$\beta_{p,\,532}(100°)$ vs. Chl a	9.19×10^{-4}	5.66×10^{-1}	0.51	12.0	49.6	176
$\beta_{p,\,532}(100°)$ vs. POC	4.24×10^{-3}	8.23×10^{-1}	0.56	**11.5**	**48.4**	93
$\beta_{p,\,532}(100°)$ vs. POM	1.75×10^{-3}	6.58×10^{-1}	0.50	13.7	57.2	151

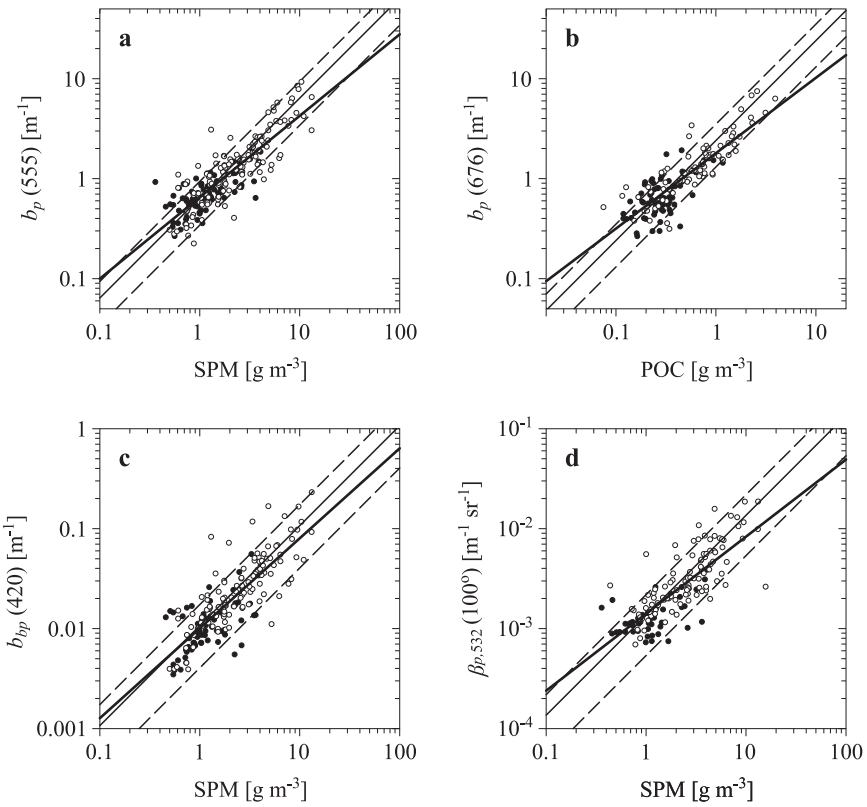

Figure 7. Relationships between a) the scattering coefficient of particles $b_p(555)$ and SPM; b) $b_p(650)$ and POC; c) the backscattering coefficient of particles $b_{bp}(420)$ and SPM; d) the particle volume scattering function $\beta_{p,\,532}(100°)$ and SPM. The data points are colour coded as in Figure 2. The thin solid lines represent graphically the corresponding average values of the constituent specific coefficients, the thin dashed lines represent the ranges of average ± SD (see Table 3), and the thick lines represent the best-fit power functions (see Table 4, p. 716)

(SD)) (the minimum and maximum of η are −5.97 and 0.184 respectively); this means that, on average, spectra of b_{bp} are much steeper than those of b_p. Average values of ${b_{bp}}^*(\lambda)$ (see row 5 of Table 4) have CV ≥ 62%. The variability is lowest for the spectral band of 420 nm (see the data points in Figure 7c, and the best-fit power function between $b_{bp}(420)$ and SPM given in row 6 of Table 5). Note that if the statistical parameters of the fits are compared, b_{bp} seems to be a less attractive proxy for SPM than b_p.

The average values of b_{bp} normalized to Chl a, POC, POM (i.e. values of ${b_{bp}}^{*(\mathrm{Chl}\ a)}(\lambda)$, ${b_{bp}}^{*(\mathrm{POC})}(\lambda)$, ${b_{bp}}^{*(\mathrm{POM})}(\lambda)$) are listed in rows 6, 7 and 8 of Table 4. The variability of these constituent-specific backscattering coefficients is much greater than that of ${b_{bp}}^*(\lambda)$ described earlier. In the

'best' spectral cases (with the lowest variability) CV = 83%, 70%, 70% and 92% for ${b_{bp}}^{*(\text{Chl } a)}(550)$, ${b_{bp}}^{*(\text{POC})}(550)$, ${b_{bp}}^{*(\text{POC})}(620)$ and ${b_{bp}}^{*(\text{POM})}(420)$ respectively. The corresponding best-fit power functions are given in rows 7, 8, 9 and 10 of Table 5. Comparison of the statistical parameters of these fits with the corresponding statistical parameters of the fits found for the scattering coefficient b_p shows that b_{bp} also appears to be a less attractive proxy than b_p for Chl a, POC or POM.

The final characteristic of light scattering by particles is the particle volume scattering function measured for a light wavelength of 532 nm $\beta_{p,532}(\theta)$, and for three scattering angles θ (100°, 125° and 150°). Figure 6c lists mass-specific particle volume scattering functions ${\beta_{p,532}}^{*}(\theta)$ (i.e. values of $\beta_{p,532}(\theta)$ normalized to SPM) for all samples. The last four rows of Table 4 give the average different constituent-specific particle volume scattering functions. CV is the lowest for the mass-specific particle volume scattering function ${\beta_{p,532}}^{*}(\theta)$. Figure 7d presents the relationship between $\beta_{p,532}(100)$ and SPM together with the best-fit power function (see row 11 in Table 5). The best power function fits for the relationships between $\beta_{p,532}(100)$ and Chl a, POC and POM are given in the last three rows of Table 5. As the statistical parameters describing these fits show, $\beta_{p,532}(100)$ does not seem to be a better proxy for any of these biogeochemical parameters (compared with the backscattering coefficient).

At this point we would like to present a brief comparison of our results concerning constituent-specific light scattering coefficients with literature data available for different coastal sea waters. For their Baltic samples, Babin et al. (2003a) reported an average mass-specific scattering coefficient ${b_p}^{*}(555)$ of 0.49 $\text{m}^2\ \text{g}^{-1}$ and its geometric standard deviation (applied as a factor) of 1.7, which gives a range of ${b_p}^{*}(555)$ between 0.29 and 0.83 $\text{m}^2\ \text{g}^{-1}$. Their average value is somewhat smaller than ours, but the range is not far from the one we found for southern Baltic samples: in fact, we obtained an average ${b_p}^{*}(555)$ of 0.64 $\text{m}^2\ \text{g}^{-1}$ and a range ($\pm$ SD) from 0.34 to 0.94 $\text{m}^2\ \text{g}^{-1}$. Also, in terms of the shape of the b_p spectrum, Babin et al. (2003a) reported that average slopes were distinctly less steep than the λ^{-1} function (in our case, as we already mentioned, the average slope was about -0.4). For the tropical coastal waters off eastern Australia Oubelkheir et al. (2006) reported an average value of ${b_p}^{*}(555)$ of 0.85 $\text{m}^2\ \text{g}^{-1}$ ($\pm$ 0.48 $\text{m}^2\ \text{g}^{-1}$) for the majority of their bay water samples. They also mentioned a much wider range of values from estuarine and offshore waters (from ca 0.5 $\text{m}^2\ \text{g}^{-1}$ to as much as 2.3 $\text{m}^2\ \text{g}^{-1}$). In another work, Stavn & Richter (2008) estimated mass-specific scattering coefficients at 555 nm for the organic fraction of their samples from the northern Gulf of Mexico to be in some cases as low as 0.32 and in others as

high as 1.2 m^2 g^{-1}. All these examples show that the variability in the mass-specific scattering coefficient $b_p{}^*$ that we recorded in the southern Baltic does not seem to be unusual. From the work of McKee & Cunningham (2006) we can also cite values of chlorophyll-specific coefficients of scattering and backscattering. For Irish Sea waters they estimated values of those coefficients for their set of organic-dominated samples. In fact they reported the average value of $b_p{}^{(\mathrm{Chl}\ a)}(555)$ to be 0.36 m^2 mg^{-1} (± 0.04 m^2 mg^{-1}), which is higher than the average we obtained for the southern Baltic (recall that we reported a value of 0.27 m^2 mg^{-1} (SD = 0.21 m^2 mg^{-1})); but when we consider ranges reported rather than average values alone they do not seem to be contradictory. In the case of the chlorophyll-specific backscattering coefficient McKee & Cunningham (2006) also reported an average value higher than that resulting from our database (their average of $b_{bp}{}^{*(\mathrm{Chl}\ a)}(470)$ was 0.005 m^2 mg^{-1} (± 0.0009 m^2 mg^{-1}), while for the closest available wavelength we reported $b_{bp}{}^{*(\mathrm{Chl}\ a)}(488)$ of 0.003 m^2 mg^{-1} (± 0.0025 m^2 mg^{-1})), but again our ranges overlap most of their data, so they too are not exclusive.

We would now like to make some final comments on the reported variability of different constituent-specific IOPs. First we would like to draw attention to the fact that some of the case-by-case variability presented here could be the result of measurement errors, inevitable in any empirical study. That is why in our analyses we have tried to present variability in terms of statistical parameters such as standard deviations and/or coefficients of variation rather than emphasizing particular values and the significance of some extreme cases. We believe that by doing so we probably stress most of the real and true part of the variability encountered in relations between the particulate constituents of seawater and their IOPs. At the same time, we are also aware that with our empirical database we cannot offer any profound physical explanation of the recorded variability in constituent-specific IOPs. This is because, as we mentioned earlier, in our studies we were not able to register one of the most important characteristics of the particle populations encountered, namely, their size distributions. It is well known that major sources of variability in particulate optical properties include the particle composition (a determinant of the particle refractive index) and the particle size distribution (Bohren & Huffman 1983, Jonasz & Fournier 2007). Unfortunately, size distribution measurements were beyond our experimental capabilities at the time when the empirical data were being gathered at sea. Such limitation is not unusual – many modern in situ optical experiments often lack size distribution measurements as they are difficult to carry out directly at sea (outside the laboratory) and on large numbers of samples. Given such a limitation, all we can offer the

interested reader is an extensive documentation of seawater IOP variability but without a detailed physical explanation of it.

3.4. Formulas for estimating particulate characteristics from IOPs

Regardless of the findings presented in the above paragraphs, i.e. documented distinct variability in relationships between particle IOPs and particle concentration parameters, which to some readers might sound rather 'negative', we attempt below to show an example of the practical outcome of our analyses. On the basis of the set of best-fit power function relationships established between selected IOPs and constituent concentrations presented earlier (summarized in Tables 3 and 5), we also tried to find the best candidates for the inverted relationships. Such relationships could be used to estimate the concentrations of certain constituents based on values of seawater optical properties measured in situ. In view of all the analyses presented earlier, one can obviously expect these inverted relations to be of a very approximate nature. But in spite of such expectations, their potential usefulness can be quantitatively appraised on the basis of analyses of the values of the mean normalized bias (MNB) and the normalized root mean square error (NRMSE). These statistical parameters have to be taken into account by anyone wishing to use these relationships in practice.

The analyses of all our data suggest that the SPM concentration can be roughly estimated, preferably on the basis of the particle scattering coefficient $b_p(555)$. The following relationship was found:

$$\mathrm{SPM} = 1.71[b_p(555)]^{0.898} . \tag{1}$$

The coefficient r^2 of that relation is 0.73 (number of observations $n = 223$), while MNB and NRMSE are 8.5% and 49.5% respectively. The latter value obviously suggests that the statistical error of such an estimate may be significant.

Analysis of r^2 for the different relationships presented in Tables 3 and 5 indicates that the best candidate for estimating Chl a from inherent optical properties would appear to be the absorption coefficient of phytoplankton pigments $a_{ph}(675)$ or $a_{ph}(440)$ (r^2 for best-fit power function relationships between Chl a and $a_{ph}(675)$ and Chl a and $a_{ph}(440)$ are 0.90 and 0.84 respectively). But since a_{ph} may be obtained as a result of time-consuming laboratory analyses of discrete seawater samples (i.e. filter pad measurements combined with the bleaching of phytoplankton pigments) rather than being retrieved directly from in situ measurements, we will now present another relationship for estimating Chl a – one based on the

particle absorption coefficient $a_p(440)$. This parameter can be retrieved, for example, from parallel in situ measurements of absorption coefficients of all non-water components and absorption coefficients of CDOM, performed with two instruments such as ac-9 or acs (WetLabs), where one of the instruments makes measurements on filtered seawater. The following formula for Chl a is then:

$$\text{Chl } a = 16.7[a_p(440)]^{1.06}$$

$$(\mathrm{r}^2 = 0.73;\ \text{MNB} = 12.4\%;\ \text{NRMSE} = 66.5\%;\ \mathrm{n} = 323). \tag{2}$$

This formula is clearly encumbered with a significantly high NRMSE; indeed, it is even higher than in equation (1) suggested for the estimation of SPM.

For estimating POC we found a simple relation based on the particle scattering coefficient $b_p(676)$ to be the most effective one:

$$\text{POC} = 0.452[b_p(676)]^{0.962}$$

$$(\mathrm{r}^2 = 0.72;\ \text{MNB} = 9.0\%;\ \text{NRMSE} = 50.0\%;\ \mathrm{n} = 148). \tag{3}$$

And to estimate POM we propose a formula based on the scattering coefficient $b_p(650)$:

$$\text{POM} = 1.49[b_p(650)]^{0.852}$$

$$(\mathrm{r}^2 = 0.72;\ \text{MNB} = 9.2\%;\ \text{NRMSE} = 56.0\%;\ \mathrm{n} = 223). \tag{4}$$

Further exploration of our database showed that in case of POM, the effective quality of its retrieval can be improved to some extent by using two different statistical relationships between POM and $b_p(650)$, based on a division of all samples into two separate classes differing from one another in particle composition. At this point we must mention that while exploring our database we found two promising statistical relationships between the composition ratio of POM/SPM and different ratios of particle IOPs (i.e. $a_p(440)/a_p(400)$ and $b_{bp}(488)/b_p(488)$), which could be useful for determining this division (see Figure 8 for the details of both relations). The first of these relationships (offering a slightly better value of $\mathrm{r}^2 - 0.44$) is based on the particle absorption ratio and takes the form

$$\frac{\text{POM}}{\text{SPM}} = 0.714\frac{a_p(440)}{a_p(400)} + 0.0296. \tag{5}$$

Regardless of the relatively low value of r^2, we think this relation may at least be used to distinguish between cases with relatively high and low POM/SPM ratios. To demonstrate the usefulness of such a relation, we

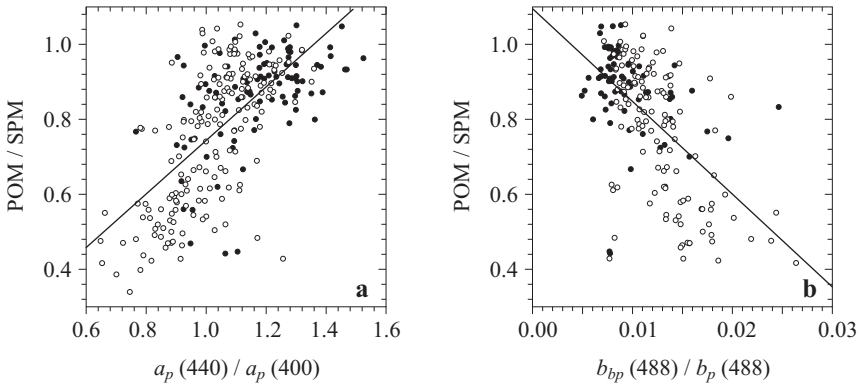

Figure 8. Relationships between a) the POM/SPM ratio and $a_p(440)/a_p(400)$ ratio; b) the POM/SPM ratio and $b_{bp}(488)/b_p(488)$ ratio. The data points are colour coded as in Figure 2. The thick solid lines represent linear regressions (equations of POM/SPM $= 0.714[a_p(440)/a_p(400)] + 0.0269$, $r^2 = 0.44$, and POM/SPM $= -24.7[b_{bp}(488)/b_p(488)] + 1.09$, $r^2 = 0.32$ respectively)

show below a two-stage algorithm for estimating POM. We took the average value of POM/SPM for our whole dataset (0.795) as the boundary value to help distinguish between the two classes of particle populations. We classified particle populations with POM/SPM > 0.795 as class I (or organic-dominated class), and particle populations with POM/SPM < 0.795 as class II (or mixed class). On the basis of this division we were able to calculate a pair of relationships similar to that in equation (2). For class I particles (organic-dominated class) the first relationship takes the form

$$\mathrm{POM} = 1.62[b_p(650)]^{0.901}$$

$$(r^2 = 0.76;\ \mathrm{MNB} = 7.4\%;\ \mathrm{NRMSE} = 45.8\%;\ n = 148), \tag{6a}$$

and for class II (mixed sample class) the second relationship is as follows:

$$\mathrm{POM} = 1.27[b_p(650)]^{0.766}$$

$$(r^2 = 0.70;\ \mathrm{MNB} = 9.5\%;\ \mathrm{NRMSE} = 57.3\%;\ n = 75). \tag{6b}$$

Having established the above relations, we construct a two-stage algorithm to estimate POM. In the first step we propose using the values of $a_p(440)$ and $a_p(400)$ and equation (5) to estimate POM/SPM, and on the basis of this estimated value, to classify our particular case as class I or class II. Then, in the second step, we can calculate the value of POM according to equation (6a) or (6b), depending on the result of the first step of the classification. Here we must bear in mind that in certain situations the first step of this procedure may mean that some cases will be erroneously

classified as class I or class II (because of the statistical nature of equation (5) used in the classification). This will obviously lead to a partial deterioration of the overall quality of the proposed two-stage procedure. Nevertheless, this overall quality may be statistically accessed in the same manner as was done in the case of the one-step procedure (i.e. equation (4)), by calculating the corresponding values of MNB and NRMSE. In fact, our two-stage procedure for estimating POM resulted in the following values: MNB = 7.9% and NRMSE = 49.4% (number of observations n = 220). This means that by using the proposed two-stage procedure instead of the simple formula given by equation (4), we obtain improved values of MNB and NRMSE (compare values of 7.9% with 9.2%, and 49.4% with 56%). That suggests that the two-stage procedure for estimating POM might be worth implementing in situations where the particle composition (in terms of POM/SPM) is expected to vary significantly.

This two-stage procedure is given only for the estimation of POM values. Admittedly, we also attempted to construct similar two-stage procedures for estimating SPM, Chl *a* and POC, but we were unable to achieve a significant improvement in the estimates compared to simple relations presented earlier (equations (1), (2) and (3)).

Finally, we have to stress once again that the formulas and procedure presented above (equations (1)–(6)) are merely examples. They were obtained as the best alternatives for estimating constituents on the basis of statistical analyses of our whole empirical data set, but were obviously not tested against any other independent dataset. These best formulas and the procedure are still characterized by small but significant systematic errors (MNB) of the order of 10%, and, most importantly, by relatively high statistical errors (NRMSE) of the order of at least 50%. As a result, their applicability is limited to only rough estimates of particulate characteristics and they should be treated with caution.

4. Summary

Our empirical material documented a high variation of the absolute values of both measures of particle concentration (e.g. 30-fold to 50-fold ranges in SPM, POM, and POC, and a 190-fold range in Chl *a*) and inherent optical properties (IOPs) (e.g. an almost 50-fold range in the absorption coefficient of particles at 440 nm, a more than 40-fold range in the scattering coefficient at 555 nm and an almost 70-fold range in the backscattering coefficient at 420 nm). Although most of the particle populations encountered were composed primarily of organic matter (av. POM/SPM = 0.795), the different particle concentration ratios suggest that the particle composition varied significantly (the respective coefficients

of variation (CVs) of POM/SPM, POC/SPM and Chl a/SPM, were 22%, 41% and 81%). The variability in the relationships between IOPs and the different measures of suspended particle concentration were also documented. We focused primarily on examining the variability of different constituent-specific IOPs (see Tables 2 and 4), and also on the determination of simple statistical best-fit relations between any given IOP value versus any constituent concentration parameter (see Tables 3 and 5). As a result we found that for southern Baltic samples an easy yet precise quantification of particle IOPs in terms of concentration of only one of the following – SPM, POM, POC or Chl a – is not achievable. Even if we consider the optical coefficients (at certain spectral bands), which show the highest possible correlation with the concentration of any constituent, we still find a large variability in such empirical relationships. For example, the mass-specific (SPM-specific) absorption coefficient at 440 nm ${a_p}^*(440)$ varies significantly (CV = 71%). In the case of the chlorophyll-specific absorption coefficient of phytoplankton at 675 nm ${a_p}^{*(\mathrm{Chl}\ a)}(675)$, CV = 29%. In another example, the mass-specific scattering coefficient at 650 nm ${b_p}^*(650)$ and the mass-specific backscattering coefficient at 420 nm ${b_{bp}}^*(420)$ have respective CVs of 46% and 62%. These examples confirm that for the southern Baltic Sea one cannot find a set of 'precise values' of constituent-specific IOPs that could be used as simple and accurate conversion factors between biogeochemical and optical parameters for marine modelling and study purposes. Examination of non-linear statistical relationships (power function fits) also confirms that an exact quantification of spectral IOPs values in terms of SPM, POM, POC or Chl a alone is not easily achievable. Regardless of the above critical findings, what we can offer as a practical outcome of our analyses is a set of approximate statistical relationships and procedures (see equations (1)–(6)). These relationships can be used in practice but only to make rough estimates of certain seawater constituent concentrations based on relatively easily measurable values of seawater IOPs. At the same time it has to be borne in mind that the application of such simplified relationships will inevitably entail statistical errors of estimation of the order of 50% or more.

Acknowledgements

We thank Sławomir Sagan for his assistance with the ac-9 instrument measurements and Dorota Burska for the analysis of samples for particulate organic carbon performed at the Institute of Oceanography (University of Gdańsk).

References

Arst H., 2003, *Optical properties and remote sensing of multicomponental water bodies*, Springer, Praxis, New York, 231 pp.

Babin M., Morel A., Fournier-Sicre V., Fell F., Stramski D., 2003a, *Light scattering properties of marine particles in coastal and open ocean waters as related to the particle mass concentration*, Limnol. Oceanogr., 48 (2), 843–859, doi:10.4319/lo.2003.48.2.0843.

Babin M., Stramski D., Ferrari G. M., Claustre H., Bricaud A., Obolensky G., Hoepffner N., 2003b, *Variations in the light absorption coefficients of phytoplankton, nonalgal particles, and dissolved organic matter in coastal waters around Europe*, J. Geophys. Res., 108 (C7), 3211, 20 pp., doi:10.1029/2001JC000882.

Bohren C. F., Huffman D. R., 1983, *Absorption and scattering of light by small particles*, Wiley, New York, 530 pp.

Bricaud A., Morel A., Babin M., Allali K., Claustre H., 1998, *Variations of light absorption by suspended particles with chlorophyll a concentration in oceanic (case 1) waters: analysis and implications for bio-optical models*, J. Geophys. Res., 103 (C13), 31033–31044, doi:10.1029/98JC02712.

Bricaud A., Stramski D., 1990, *Spectral absorption coefficients of living phytoplankton and nonalgal biogenous matter: a comparison between the Peru upwelling area and the Sargasso Sea*, Limnol. Oceanogr., 35 (3), 562–582.

Dana D. R., Maffione R. A., 2002, *Determining the backward scattering coefficient with fixed-angle backscattering sensors – revisited*, Ocean Optics XVI Conf., 18–22 November, Santa Fe, New Mexico, 9 pp.

Dera J., 1992, *Marine physics*, Elsevier, Amsterdam, 516 pp.

Dera J., 2003, *Marine physics*, 2nd edn., PWN, Warszawa, 541 pp., (in Polish).

Dera J., Woźniak B., 2010, *Solar radiation in the Baltic Sea*, Oceanologia, 52 (4), 533–582.

Gallegos C. L., Jordan T. E., Hines A. H., Weller D. E., 2005, *Temporal variability of optical properties in a shallow, eutrophic estuary: seasonal and interannual variability*, Estuar. Coast. Shelf Sci., 64 (2–3), 156–170, doi:10.1016/j.ecss.2005.01.013.

Gordon H. R., 2002, *Inverse methods in hydrologic optics*, Oceanologia, 44 (1), 9–58.

Gordon H. R., Brown O. B., Jacobs M. M., 1975, *Computed relationships between inherent and apparent optical properties of a flat, homogeneous ocean*, Appl. Optics, 14 (2), 417–427, doi:10.1364/AO.14.000417.

Green R. E., Sosik H. M., Olson R. J., 2003, *Contributions of phytoplankton and other particles to inherent optical properties in New England continental shelf waters*, Limnol. Oceanogr., 48 (6), 2377–2391, doi:10.4319/lo.2003.48.6.2377.

HOBI Labs (Hydro-Optics, Biology, and Instrument. Lab. Inc.), 2008, *HydroScat-4 Spectral Backscattering Sensor. USER'S MANUAL*, Rev. 4., June 15 2008, 65 pp.

Jonasz M., Fournier G. R., 2007, *Light scattering by particles in water. Theoretical and experimental foundations*, Acad. Press, Amsterdam, 704 pp.

Kaczmarek S., Stramski D., Stramska M., 2003, *The new pathlength amplification factor investigation*, Abstract Publ., Baltic Sea Sci. Congr., Helsinki, p. 149.

Kirk J. T. O., 1994, *Light and photosynthesis in aquatic ecosystems*, Cambridge Univ. Press, London, New York, 509 pp., doi:10.1017/CBO9780511623370.

Maffione R. A., Dana D. R., 1997, *Instruments and methods for measuring the backward-scattering coefficient of ocean waters*, Appl. Optics, 36 (24), 6057–6067, doi:10.1364/AO.36.006057.

McKee D., Cunningham A., 2006, *Identification and characterization of two optical water types in the Irish Sea from in situ inherent optical properties and seawater constituents*, Estuar. Coast. Shelf Sci., 68 (1–2), 305–316, doi:10.1016/j.ecss.2006.02.010.

Mitchell B. G., 1990, *Algorithm for determining the absorption coefficient of aquatic particulates using the quantitative filter technique*, Proc. SPIE, Vol. 1302, 137–148, doi:10.1117/12.21440.

Morel A., 1974, *Optical properties of pure water and pure sea water*, [in:] *Optical aspects of oceanography*, M. G. Jerlov & E. S. Nielsen (eds.), Acad. Press, New York, 1–24.

Morel A., Bricaud A., 1981, *Theoretical results concerning light absorption in a discrete medium, and application to specific absorption of phytoplankton*, Deep-Sea Res., 28 (11), 1375–1393, 10.1016/0198-0149(81)90039-X.

Morel A., Maritorena S., 2001, *Bio-optical properties of oceanic waters: a reappraisal*, J. Geophys. Res., 106 (C4), 7163–7180, doi:10.1029/2000JC000319.

Morel A., Prieur L., 1977, *Analysis of variations in ocean color*, Limnol. Oceanogr., 22 (4), 709–722, doi:10.4319/lo.1977.22.4.0709.

Oubelkheir K., Clementson L. A., Webster I. T., Ford P. W., Dekker A. G., Radke L. C., Daniel P., 2006, *Using inherent optical properties to investigate biogeochemical dynamics in a tropical macrotidal coastal system*, J. Geophys. Res., 111, C07021, 15 pp., doi:10.1029/2005JC003113.

Pearlman S. R., Costa H. S., Jung R. A., McKeown J. J., Pearson H. E., 1995, *Solids (section 2540)*, [in:] *Standard methods for the examination of water and wastewater*, A. D. Eaton, L. S. Clesceri & A. E. Greenberg (eds.), APHA, Washington, D.C., 253–254.

Pegau W. S., Gray D., Zaneveld J. R. V., 1997, *Absorption and attenuation of visible and near-infrared light in water: dependence on temperature and salinity*, Appl. Optics, 36 (24), 6035–6046, doi:10.1364/AO.36.006035.

Snyder W. A., Arnone R. A., Davis C. O., Goode W., Gould R. W., Ladner S., Lamela G., Rhea W. J., Stavn R., Sydor M., Weidemann A., 2008, *Optical scattering and backscattering by organic and inorganic particulates in U.S. coastal waters*, Appl. Opt., 47 (5), 666–677, doi:10.1364/AO.47.000666.

Stavn R. H., Richter S. J., 2008, *Biogeo-optics: particle optical properties and the partitioning of the spectral scattering coefficient of ocean waters*, Appl. Optics, 47 (14), 2660–2679, doi:10.1364/AO.47.002660.

Stoń-Egiert J., Kosakowska A., 2005, *RP-HPLC determination of phytoplankton pigments-comparison of calibration results for two columns*, Mar. Biol., 147 (1), 251–260, doi:10.1007/s00227-004-1551-z.

Stoń-Egiert J., Łotocka M., Ostrowska M., Kosakowska A., 2010, *The influence of biotic factors on phytoplankton pigment composition and resources in Baltic ecosystems: new analytical results*, Oceanologia, 52 (1), 101–125.

Stramska M., Stramski D., Kaczmarek S., Allison D. B., Schwarz J., 2006, *Seasonal and regional differentiation of bio-optical properties within the north polar Atlantic*, J. Geophys. Res., 111, C08003, 16 pp., doi:10.1029/2005JC003293.

Tassan S., Ferrari G. M., 1995, *An alternative approach to absorption measurements of aquatic particles retained on filters*, Limnol. Oceanogr., 40 (8), 1358–1368, doi:10.4319/lo.1995.40.8.1358.

Tassan S., Ferrari G. M., 2002, *A sensitivity analysis of the 'Transmittance-Reflectance' method for measuring light absorption by aquatic particles*, J. Plankton Res., 24 (8), 757–774, doi:10.1093/plankt/24.8.757.

Trenberth K. E. (ed.), 1992, *Climate system modeling*, Cambridge Univ. Press, London–New York, 788 pp.

Vantrepotte V., Brunet C., Mériaux X., Lécuyer E., Vellucci V., Santer R., 2007, *Bio-optical properties of coastal waters in the Eastern English Channel*, Estuar. Coast. Shelf Sci., 72 (1–2), 201–212, doi:10.1016/j.ecss.2006.10.016.

Woźniak B., Dera J., Ficek D., Majchrowski R., Kaczmarek S., Ostrowska M., Koblentz-Mishke O. I., 1999, *Modeling the influence of acclimation on the absorption properties of marine phytoplankton*, Oceanologia, 41 (2), 187–210.

Woźniak S. B., Stramski D., Stramska M. Reynolds R. A., Wright V. M., Miksic E. Y., Cichocka M., Cieplak A. M., 2010, *Optical variability of seawater in relation to particle concentration, composition, and size distribution in the nearshore marine environment at Imperial Beach, California*, J. Geophys. Res., 115, C08027, 19 pp., doi:10.1029/2009JC005554.

Zaneveld J. R. V., Kitchen J. C., Moore C., 1994, *The scattering error correction of reflecting-tube absorption meters*, Proc. SPIE Int. Soc. Opt. Eng., 2258, 44–55.